

Title: Semienzymatic cyclization of disulfide-rich peptides using sortase A*

Xinying Jia^{†‡1}, Soohyun Kwon^{†1}, Ching-I Anderson Wang[‡], Yen-Hua Huang[‡], Lai Y. Chan[‡], Chia Chia Tan[‡], K. Johan Rosengren^{§2}, Jason P. Mulvenna^{†2}, Christina I. Schroeder^{‡3}, David J. Craik^{‡3,4}

[†]QIMR Berghofer Medical Research, Brisbane 4000, Qld, Australia.

[‡]The University of Queensland, Institute for Molecular Bioscience, Brisbane 4072, Qld, Australia

[§]The University of Queensland, School of Biomedical Sciences, Brisbane 4072, Qld, Australia

Running title: Sortase A as a tool for cyclizing disulfide-rich peptides*

To whom correspondence should be addressed. David J. Craik or Christina I. Schroeder, The University of Queensland, Institute for Molecular Bioscience, Brisbane 4072, Qld, Australia. Tel.: 61-7-33462019; Fax: 61-7-33462101; E-mail: d.craik@imb.uq.edu.au or c.schroeder@imb.uq.edu.au.

*These two authors contributed equally to this work.

Keywords: cyclic peptides, cyclotides, enzymatic cyclization, sortase A, kalata B1

Background: Sortase A (SrtA) is a transpeptidase capable of catalyzing the formation of amide bonds.

Results: SrtA was used to backbone cyclize disulfide-rich peptides, including kalata B1, α -conotoxin Vc1.1 and SFTI-1.

Conclusion: SrtA-mediated cyclization is applicable to small disulfide-rich peptides.

Significance: SrtA-mediated cyclization is an alternative to native chemical ligation for the cyclization of small peptides of therapeutic interest.

ABSTRACT

Disulfide-rich cyclic peptides have generated great interest in the development of peptide-based therapeutics due to their exceptional stability towards chemical, enzymatic or thermal attack. In particular, they have been used as scaffolds onto which bioactive epitopes can be grafted to take advantage of the favorable biophysical properties of disulfide-rich cyclic peptides. To date, the most commonly used method for the head-to-tail

cyclization of peptides has been native chemical ligation. In recent years, however, enzyme-mediated cyclization has become a promising new technology due to its efficiency, safety and cost-effectiveness. Sortase A (SrtA) is a bacterial enzyme with transpeptidase activity. It recognizes a C-terminal penta-amino acid motif 'LPXTG' and cleaves the amide bond between Thr and Gly to form a thioacyl-linked intermediate. This intermediate undergoes nucleophilic attack by an N-terminal poly-Gly sequence to form an amide bond between the Thr and N-terminal Gly. Here, we demonstrate that sortase A can successfully be used to cyclize a variety of small disulfide-rich peptides, including the cyclotide kalata B1, α -conotoxin Vc1.1 and sunflower trypsin inhibitor 1 (SFTI-1). These peptides range in size from 14 to 29 amino acids and respectively contain three, two or one disulfide bond within their head-to-tail cyclic backbones. Our findings provide proof-of-concept for the potential broad applicability of enzymatic cyclization of disulfide-rich

This is a post-print version of the following article: Jia, Xinying, Kwon, Soohyun, Wang, Ching-I Anderson, Huang, Yen-Hua, Chan, Lai Y., Tan, Chia Chia, Rosengren, K. Johan, Mulvenna, Jason P., Schroeder, Christina I. and Craik, David J. (2014) Semienzymatic cyclization of disulfide-rich peptides using sortase A. *Journal of Biological Chemistry, Papers in Press* : 1-25.

peptides with therapeutic potential.

INTRODUCTION

Disulfide-rich cyclic peptides are generating great interest in the field of drug design because of their remarkable stability towards enzymatic, thermal or chemical attack (1). Additionally, anecdotal evidence of some of them being orally bioavailable in indigenous medicine applications (2) has recently received support from studies demonstrating oral activity of engineered cyclic peptides in animal pain models (3,4). Several classes of cyclic peptides, including the sunflower trypsin inhibitors and cyclotides have now been discovered in a variety of plant species (5). In addition to the plant-derived cyclic peptides, disulfide-rich peptides isolated from cone snails, including α -conotoxins, have successfully been cyclized (3,6) and are showing promise as potential treatments for neuropathic pain (3).

Sunflower trypsin inhibitor 1 (SFTI-1) comprises 14 amino acids with a head-to-tail cyclized backbone. It was isolated from sunflower seeds and can specifically inhibit trypsin activity at 0.1 nM (7), which makes it the smallest and most potent serine proteinase inhibitor known. It was also reported to have inhibition activity against the epithelial serine protease matriptase at subnanomolar concentration (8). Its structure consists of two antiparallel β -strands connected by an extended loop and a sharp hairpin turn caused by a *cis*-proline residue. The β -strands are constrained by a single disulfide bond, which stabilizes the molecule and divides it into two regions – the active site loop and cyclization loop (7) (Fig. 1A).

Cyclotides are characterized by the combination of head-to-tail backbone cyclization and six conserved Cys residues forming a distinctive disulfide linkage pattern in which one disulfide bond passes through a ring formed by two other disulfide bonds (9,10) (Fig. 1B). The combination of a cyclic backbone and a knotted arrangement of three disulfide bonds is known as the cyclic cystine knot (CCK) motif and this motif is

believed to be responsible for their exceptional stability towards chemical, enzymatic, or thermal degradation (1). Although thought to have a natural function as defense molecules in plants via their pesticidal activities (11-13), cyclotides possess a range of pharmaceutically interesting biological activities, including uterotonic (2), anti-HIV (14), antimicrobial (15), insecticidal (11,16) activities, and are cytotoxic to tumour cells (17,18). Thousands of cyclotides are thought to exist in nature and more than 250 sequences have been described so far (<http://www.cybase.org.au>) (19), making them one of the most abundant plant protein families discovered.

Cyclotides are able to accommodate the synthetic introduction of a range of biologically active sequence motifs in the backbone loops between the conserved Cys residues while retaining thermal, chemical and enzymatic stability. This tolerance to sequence substitutions makes them ideal scaffolds for the development of stable peptide-based drugs incorporating epitopes of therapeutic value. For example, a kB1 hybrid, with an anti-angiogenic epitope incorporated into loop 3, combined anti-angiogenic activity with the native stability of kB1 (20). Likewise, molecules possessing activity against foot-and-mouth disease (21), inhibitory activity against β -tryptase and human leukocyte elastase (22), angiogenic activity (23), and the ability to antagonize intracellular p53 degradation (24) have also been achieved by grafting relevant bioactive epitopes into the cyclotides MCoTI-I or MCoTI-II. The capacity to target intracellular sites is consistent with a range of recent biophysical studies demonstrating the ability of disulfide-rich cyclic peptides to internalize into cells (24-28).

As well as being valuable scaffolds, naturally occurring cyclic peptides such as cyclotides and SFTI-1 have inspired the concept of using artificial head-to-tail backbone cyclization as a stabilizing strategy for peptides and proteins of therapeutic interest (3,6). For example, Clark *et al.* showed that cyclization of α -conotoxin Vc1.1, a potential neuropathic pain treatment, engendered it

This is a post-print version of the following article: Jia, Xinying, Kwon, Soohyun, Wang, Ching-I Anderson, Huang, Yen-Hua, Chan, Lai Y., Tan, Chia Chia, Rosengren, K. Johan, Mulvenna, Jason P., Schroeder, Christina I. and Craik, David J. (2014) Semienzymatic cyclization of disulfide-rich peptides using sortase A. *Journal of Biological Chemistry, Papers in Press* : 1-25.

with orally activity (3). Thus, great interest has been shown in the development of cost-effective and efficient methods for the N- to C-terminal backbone cyclization of synthesized or expressed proteins (29,30). In the case of cyclic Vc1.1 (cVc1.1) the termini of the naturally occurring 16 residue peptide were covalently linked using a 6 amino acid linker as illustrated in Fig. 1C (3).

Currently, the most widely-used strategy for backbone cyclization of synthetic peptides is native chemical ligation (NCL) (31,32), which utilizes an N-terminal cysteine and a functionalized C-terminus to form a thioester-linked intermediate that undergoes an S, N acyl migration to form a native peptide bond (32). In general peptides are synthesized using solid phase peptide synthesis (SPPS), using either *t*-butoxycarbonyl (Boc) or fluorenylmethoxycarbonyl (Fmoc) protection. Despite the usefulness of NCL for splicing or cyclizing protein, there is still a demand for alternative methods of amide bond formation that are chemoselective, rapid, cheap, safe and waste-free (30). Moreover, the requirement for an N-terminal cysteine and a C-terminal thioester in NCL is not always compatible with Fmoc SPPS or recombinant expression. Accordingly, a number of different approaches to backbone cyclization have been developed (29), including expressed protein ligation (EPL) (33,34), intein-mediated protein trans-splicing (35) and genetic code reprogramming (36).

Recently, a family of thiol-containing transpeptidases, known as the sortases, were found to successfully cyclize linear proteins (37-40). Sortases are found in most Gram-positive bacteria where their primary function is to attach surface proteins to the bacterial cell wall (41). This ligation reaction has been exploited for a variety of protein engineering purposes, in most cases utilizing sortase A (SrtA) from *Staphylococcus aureus* (42). SrtA recognizes a 5-residue sequence motif, LPXTG (X = any residue), and cleaves the peptide bond between the Thr and Gly residues forming an acyl enzyme intermediate between a

cysteine at the active site of SrtA and the carboxylate at the truncated C terminus of the substrate (43,44). Although in a natural system this covalent intermediate is resolved by nucleophilic attack from a pentaglycine side chain in a peptidoglycan precursor, a variety of glycine-based nucleophiles can activate SrtA-catalyzed transpeptidation (38). The result is the efficient attachment of various moieties to the protein substrates and it has been applied to site-specific protein labelling (45), PEGylation (46), protein thioester generation (47) and protein-protein fusion (48). When such glycine-based nucleophiles originate from the N-terminus of the substrate, intramolecular transpeptidation reactions occur to yield covalently closed (circular) polypeptides by amide bond formation between the two termini (38-40). So far this approach has been examined only for a limited number of possible substrates and has not been explored for disulfide-rich peptides.

In the current study we demonstrate the efficient enzymatic cyclization of disulfide-rich peptides, including SFTI-1, cVc1.1 and kalata B1 (kB1), containing one, two or three disulfide bonds, respectively, by SrtA without the need for a thioester linker and using Fmoc chemistry. This study provides a proof-of-concept that SrtA mediated ligation can be utilized to cyclize disulfide-rich peptides ranging from the simple one-disulfide containing SFTI-1 to the complex cyclic cystine knot containing cyclotide structure of kB1 while retaining the native disulfide bond connectivity that is vital for the stability of these proteins. Fig. 1D summarizes the cyclization strategy for kB1.

EXPERIMENTAL PROCEDURES

Peptide synthesis- The linear peptides-[GGG]kB1[TGG], [G]Vc1.1[GLPETGGS], and [GG]SFTI-1[LPETGG] were synthesized by solid-phase peptide synthesis using an automatic peptide synthesizer (Symphony®, Protein technologies, Inc.) following standard 9-fluorenylmethoxycarbonyl (Fmoc) chemistry on a

This is a post-print version of the following article: Jia, Xinying, Kwon, Soohyun, Wang, Ching-I Anderson, Huang, Yen-Hua, Chan, Lai Y., Tan, Chia Chia, Rosengren, K. Johan, Mulvenna, Jason P., Schroeder, Christina I. and Craik, David J. (2014) Semienzymatic cyclization of disulfide-rich peptides using sortase A. *Journal of Biological Chemistry, Papers in Press* : 1-25.

2-chlorotrityl chloride resin. Acetamidomethyl (Acm) protecting groups were used on Cys4 and Cys17 of [G]Vc1.1[GLPETGGGS] for selective disulfide bond (Cys^{II}-Cys^{IV}) formation. Cleavage of the peptide from the resin was achieved using trifluoroacetic acid (TFA):triisopropylsilane (TIPS):water=95:2.5:2.5 at room temperature (RT) for 2 h. The TFA was evaporated, and the peptide was precipitated with ice-cold diethyl-ether, and dissolved in 50% acetonitrile (ACN) containing 0.05% TFA and lyophilized. Wild type Vc1.1 and SFTI-1 were prepared as described previously (3,49).

SrtA expression- The plasmid of and recombinant expression protocol for *Staphylococcus aureus* SrtA, which comprises the catalytic domain (residues 60 to 206 with a N-terminal hexahistidine tag) was obtained from and as described by Popp *et al.* (50). Briefly, an overnight culture of *Escherichia coli* BL21 (DE3) transformed with SrtA plasmid was cultured in the presence of kanamycin (50 µg/mL) until OD600 reaches ~0.7. The protein expression was induced by adding isopropyl β-D-thiogalactopyranoside (IPTG) to a final concentration of 1 mM for 3 h at 37°C. The cells were then harvested by centrifugation at 7000 g at 4°C for 10 min. Cells were then resuspended in ice-cold lysis buffer (50 mM Tris-HCl, pH 8.0, 150 mM NaCl, 25 mM imidazole, and 10% glycerol) and lysed by passing through a cell disrupter (TS Series Bench Top, www.constantsystems.com) operating at 26 kpsi. The cell debris was removed by centrifugation at 12,000 g at 4°C for 30 min. The lysate was subjected for immobilised metal ion affinity chromatography using a 5 mL Ni-NTA FF column (GE healthcare, Uppsala, Sweden). The column was washed extensively with lysis buffer after sample loading and SrtA was eluted with a linear gradient over 10 column volume using elution buffer (50 mM Tris-HCl, pH 8.0, 150 mM NaCl, 500 mM imidazole). Fractions containing SrtA were buffer exchanged (50 mM Tris-HCl, 150 mM NaCl, and 10% glycerol) concentrated by using a centrifugal concentrator (<10 kDa). The SrtA was

then stored at -80°C until further use. The protein concentration was calculated by its extinction coefficient at 280 nm. (<http://web.expasy.org/protparam/>).

Oxidative folding- The linear precursor[GGG]kB1[TGG] was oxidized in 50% isopropyl alcohol (v/v)/0.1 M NH₄HCO₃ with 1 mM reduced glutathione at pH 8 for 20 h at room temperature (51). The progress of oxidation was monitored by analytical reversed-phase high performance liquid chromatography (RP-HPLC) with a gradient from 0 to 50% ACN (0.05% TFA) in 50 min at a flow rate of 0.3 mL/min using an analytical C18 column (Agilent ZORBAX 300SB-C18, 5 µm 2.1x150 mm). The oxidation yield was calculated based on HPLC profile. The mixture was then purified by RP-HPLC using a 0.5% gradient and the molecular weight was confirmed by mass spectrometry. Native kB1 was isolated from *Oldenlandia affinis* as described previously (9,52).

Both linear precursor [G]Vc1.1[GLPETGGGS] and cyclic reduced [G]Vc1.1[GLPET] were oxidized in 0.1 M NH₄HCO₃ at 0.1 mg/mL concentration for 24 h to form disulfide bond Cys^I-Cys^{III}. Purified Vc1.1 (both linear and cyclic) with one disulfide bond was then dissolved in 50% acetic acid to a final concentration of 0.5 mg/mL under N₂. Excess iodine dissolved (10 equivalents with respect to the Acm-protected Cys) in 50% acetic acid was added until the colour of reaction became yellow and the reaction was left at RT for 24 h. The reaction was quenched by addition of ascorbic acid until the solution became colourless followed by RP-HPLC purification using a gradient of 0-60% acetonitrile in 60 min.

Cyclization- The concentration of modified kB1 was determined by its molar extinction coefficient at 280 nm using NanoDrop2000c (Thermo Scientific). Linear oxidized [GGG]kB1[TGG] and linear precursor [GG]SFTI-1[LPETGG] (150 µM) were incubated with SrtA (50 µM) in the reaction buffer (50 mM Tris, pH 7.5, 150mM NaCl, 10mM CaCl₂) at 37°C until the reaction was completed. The cyclization progress was monitored using RP-

This is a post-print version of the following article: Jia, Xinying, Kwon, Soohyun, Wang, Ching-I Anderson, Huang, Yen-Hua, Chan, Lai Y., Tan, Chia Chia, Rosengren, K. Johan, Mulvenna, Jason P., Schroeder, Christina I. and Craik, David J. (2014) Semienzymatic cyclization of disulfide-rich peptides using sortase A. *Journal of Biological Chemistry, Papers in Press* : 1-25.

HPLC with a gradient from 0 to 50% ACN (0.05% TFA) in 50 min at a flow rate of 1 mL/min using an analytical C18 column (GraceSmartTM RP18, 5 μ m 4.6x150 mm). After completion of cyclization the reaction was loaded to semi-preparative C18 column (Phenomenex, Jupiter 5UC18, 300 \AA , 250x10.0 nm, 5 μ m), eluted with a gradient from 36 to 45% ACN (0.05% TFA) in 30 min at a flow rate of 3 mL/min. The molecular mass of purified cyclo-[GGG]kB1[T] was confirmed by Matrix-assisted laser desorption/ionization time of flight (MALDI-TOF). The fractions showing the correct mass were lyophilized for further assays. The concentration of Vc1.1 was also determined as described above. 10 μ M linear precursor [G]Vc1.1[GLPETGGS] was incubated with 0.2 μ M SrtA in the reaction buffer containing 10 mM TCEP for 24 h at 4°C. SrtA was then removed from the sample using a 5 mL Ni-NTA FF column (GE healthcare, Uppsala, Sweden) and the flow-through containing cyclic reduced [G]Vc1.1[GLPET] was collected and purified by RP-HPLC for oxidation.

As there are no aromatic residue available, the concentration of SFTI-1 was determined at 214 nm using the NanoDrop2000c (Thermo Scientific) UV-Vis function with the extinction coefficient calculated based on the equation of $\epsilon_{214nm}=(n_{AA}-1+n_N+n_Q)2846+n_F7200+n_H6309+n_W22735+n_Y575$ (53). 150 μ M [GG]SFTI-1[LPETGG] and 50 μ M SrtA was incubated in the reaction buffer at 37°C with pH adjusted to 8.5 to form disulfide bond at the same time. The progress of cyclization was monitored using analytical RP-HPLC with a gradient from 0 to 50% ACN (0.05% TFA) in 50 min at a flow rate of 1 mL/min using an analytical C18 column (GraceSmartTM RP18, 5 μ m 4.6x150 mm).

Nuclear magnetic resonance analysis- cyclo-[GGG]kB1[T] was dissolved in 90% H₂O/10% D₂O (v/v) or 100 % D₂O to a final concentration of 1 mM and pH 6.1 (54). Cyclo-[G]Vc1.1[GLPET] and cyclo-[GG]SFTI-1[LPET] were dissolved in 90% H₂O/10% D₂O (v/v) to a final concentration of ~1 mM and pH 3.1. All two-

dimensional (2D) nuclear magnetic resonance (NMR) spectra were acquired at 298 K. Spectra recorded for assignments and H α secondary chemical shifts analysis included TOCSY with a 80 ms mixing time and NOESY with a 200 ms mixing time. All spectra were acquired on a Bruker Avance 600 MHz NMR spectrometer equipped with a cryogenically cooled probe (Bruker, Karlsruhe, Germany). Water suppression for 2D TOCSY and 2D NOESY were achieved by using excitation sculpting (55). Spectra were recorded with 2048 data points in the direct F_2 dimension and 600 increments in the indirect F_1 dimension. Additional spectra recorded for cyclo-[GGG]kB1[T] to be used in full structure calculations were NOESY with 100 ms mixing time as well as E.COSY (56), DQF-COSY as well as ¹³C-HSQC to produce the carbon chemical shifts. All spectra were processed using Topspin (Bruker) and analysed by CCPNMR (57) and Xeasy (58). The temperature coefficients were determined from recording TOCSY spectra from 283 to 303 K in steps of 10 K. Chemical shifts were referenced to internal 2, 2-dimethyl-2-silapentane-5-sulfonate (DSS) at 0.0 ppm (59). The peaks in the NOESY spectra with mixing times of 100 ms and 200 ms were manually picked and intra-residual and sequential NOEs were assigned followed by a full list of inter-proton distance being generated from chemical shifts and NOE intensities using the AUTO function in CYANA (tolerances used for CYANA were set to 0.02 ppm for both indirect and direct ¹H dimension) (60). Several rounds of AUTO including additional restraints such as disulfide bonds, hydrogen bonds and dihedral-angle restraints derived from TALOS+ were run to ensure correct peak assignment. H α , HN, C α , C β chemical shifts derived from ¹H-¹H NOESY and ¹H-¹³C-HSQC were used to generate ϕ and ψ backbone dihedral angles using TALOS+ (61). The ANNEAL function in CYANA was used to perform 10000 steps torsion angle dynamics to generate an ensemble from which 20 with the lowest penalty function were chosen for further analysis. Several

This is a post-print version of the following article: Jia, Xinying, Kwon, Soohyun, Wang, Ching-I Anderson, Huang, Yen-Hua, Chan, Lai Y., Tan, Chia Chia, Rosengren, K. Johan, Mulvenna, Jason P., Schroeder, Christina I. and Craik, David J. (2014) Semienzymatic cyclization of disulfide-rich peptides using sortase A. *Journal of Biological Chemistry, Papers in Press* : 1-25.

rounds of ANNEAL were run to resolve distance and dihedral constraints violations. Using protocols from the RECOORD database (62), 50 structures were calculated using CNS (63) with force fields distributed with Haddock 2.0 (64) and refined in a water shell (65) as previously described (66). A set of 20 structures with no NOE violations of greater than 0.3 Å and dihedral violations greater than 3.0 degrees was chosen for MolProbity analysis (67). MOLMOL (68) was used for generating figures and final superimposition.

Hemolytic activity assay on [GGG]kB1[T]- The hemolytic assay was conducted as described previously (69). Briefly, erythrocytes were isolated from human blood and washed in phosphate-buffered saline (PBS, pH 7.4) with repeated centrifugation at 1,500 x g. The hemolytic activities of cyclo-[GGG]kB1[T], linear oxidized [GGG]kB1[TGG] and kB1 were determined with eight concentration points of from 300 µM to 1.17 µM by serial dilution with a 2-fold interval with a final volume of 20 µL per well in a 96-well plate. Triton X-100 solution (1%, v/v, 20 µL) was used as a positive control to achieve the 100% lysis, and PBS solution (20 µL) a negative control. 100 µL of erythrocyte stock solution was added to each well and incubated at 37°C for 1 h. After centrifugation of intact cells from the 96-well plate, the supernatant of each well was measured by visual absorption spectroscopy at 415 nm. Each experiment was performed in triplicate.

Serum stability assay on [GGG]kB1[T]- The stability of cyclo-[GGG]kB1[T] in human serum was evaluated using a method described previously (23). Briefly, human serum from male AB plasma (Sigma-Aldrich) was centrifuged at 17,000g for 10 minutes to remove the lipid component. The resultant supernatant was collected and incubated for 15 minutes at 37°C before the assay. Cyclo-[GGG]kB1[T], linear oxidized [GGG]kB1[TGG] and kB1 were tested at a final concentration of 20 µM. Stock solutions of peptides were diluted 1:10 with human serum whereas the dilution with PBS was negative

controls and a linear 12-mer peptide tested in parallel was served as a positive control of the peptidase activity of the serum. Controls and test peptides were incubated at 37°C and 40 µL of samples were taken for measurements at time points of 0, 1, 2, 3, 5, 8, 11, and 24 h. Serum proteins in samples were denatured with 40 µL 6 M urea at 4°C for 10 minutes and precipitated with additional 40 µL 20% trichloroacetic acid at 4°C for 10 minutes. The supernatant containing peptides was recovered by centrifugation at 17,000 g for 10 minutes. 100 µL of supernatant from each time point of the serum-treated and PBS-treated (control) peptides was injected and analysed in triplicate on an analytical RP-HPLC column (Phenomenex) at a flow rate of 0.3 mL/min with a gradient of 0 to 50% ACN over 50 minutes. The retention time for each peptide was determined by PBS control at the 0 time point. The stability of each peptide at each time point was calculated as the percentage of the integrated peak area of the serum-treated peptide over that of the 0-hour serum-treated peptide on RP-HPLC at 215 nm.

RESULTS

Protein production and purification- Linear precursors, with a SrtA recognition motif (LPXTG) at the C-terminus and an oligoglycine motif at the N-terminus (full sequence [GGG]kB1[TGG]: **GGGCGETCVGGTCNTPGCTCSWPVCTRNLGLPVTGG**, [G]Vc1.1[GLPETGGS]: **GGCCSDPRCNYDHPEICGLPETGGS**, and [GG]SFTI-1[LPETGG]: **GGGRCTKSIPPICFPDLPETGG**, with the native sequence in bold), were assembled using automated Fmoc chemistry, cleaved from the resin with TFA and purified using RP-HPLC. No oxidation of cysteine residues was observed during the purification process, as determined using mass spectrometry. The molecular mass and purity were confirmed using mass spectrometry and analytical RP-HPLC, respectively.

Oxidation and cyclization of [GGG]kB1[TGG]- The oxidative folding of the linear precursor [GGG]kB1[TGG] was monitored by RP-HPLC

(Fig. 2A) and the yield of correctly folded product was ~27% based on RP-HPLC peak integration. Following oxidative folding, linear [GGG]kB1[TGG] was purified by RP-HPLC and the correct folding was confirmed by NMR analysis (data not shown). For completeness, the stability of native kB1 in the SrtA reaction buffer was confirmed by the unchanged peak area in RP-HPLC analysis after incubation of the native form for 24 h (data not shown).

In preliminary experiments two approaches were used to obtain oxidized, cyclic kB1 using SrtA mediated cyclization. First, linear reduced [GGG]kB1[TGG] was cyclized using the SrtA reaction buffer but with the addition of 2 mM of the reducing agent TCEP. The peptide was then oxidized after completion of the cyclization reaction. Second, the linear peptide [GGG]kB1[TGG] was oxidized prior to cyclization with SrtA, which proceeded without the addition of reducing agent to the reaction buffer. Cyclization prior to oxidation resulted in higher yields of cyclic reduced peptide as determined by RP-HPLC (~80%, data not shown), but subsequent oxidative refolding yielded several isomers (<10% yield for each isomer, data not shown), presumably due to misfolding during the oxidation reaction. Oxidation prior to cyclization resulted in a predominance of correctly folded peptide and this approach was therefore used for subsequent experiments.

Cyclization of 150 μ M of linear oxidized [GGG]kB1[TGG] with 50 μ M SrtA was monitored over 24 h using RP-HPLC (Fig. 2B). The reaction was not extended beyond 24 h due to the possibility of a competing hydrolysis reaction in which SrtA irreversibly hydrolyzes the LPVTG motif (70). After 24 h, ~49% of linear, oxidized [GGG]kB1[TGG] was converted to the cyclic product (highlighted in Fig. 2B). MALDI-TOF analysis of the highlighted peak fraction showed a monoisotopic mass (3162.92 Da) corresponding to that of cyclo-[GGG]kB1[T] (Fig. 2B), which was purified to >95% purity. Interestingly, the elution time of this peak (40.8 min) was similar to that of

native kB1 (Fig. 2C) despite the additional amino acids in the sequence. Apart from this peak, two other peaks, at approximately 37 min and 40 min, appeared to be intermediate species in the cyclization reaction as their abundance over time was negatively correlated with the abundance of correctly folded cyclo-[GGG]kB1[T] (Fig. 2B). A small peak appearing at approximately 42.8 min contained a peptide with the mass corresponding to that of cyclo-[GGG]kB1[T]. This peak also increased during the course of the experiment and is most probably an alternatively folded form of the peptide (Fig. 2B).

Characterization of the cyclo-[GGG]kB1[T] by NMR- The NMR signals of cyclo-[GGG]kB1[T] were well-dispersed in the amide proton region, indicating the peptide is folded and has a well-defined structure. The individual amino acid spin systems were readily assigned using the sequential assignment procedure based on TOCSY and NOESY spectra (71). Cyclization was confirmed based on observation of a sequential α H_i-HN_{i+1} NOE between Thr30 and Gly31, indicative of the amide linkage of the C-terminal LPVT and N-terminal GGG motif (Fig. 3).

Chemical shifts are extremely sensitive to the local chemical environment, and H α chemical shifts were thus used to compare the structure of cyclo-[GGG]kB1[T] to native kB1. Overall, the chemical shift differences between the two molecules are minimal (Fig. 3). With the exception of residues 1 and 27-33 (numbering system in Fig. 3), which are in loop 6 and either very close to or part of the SrtA sorting motif, no other cyclo-[GGG]kB1[T] residue exhibited significant deviations from the corresponding residue in native kB1. The very small shifts from random coil values for residues 1 and 27-33 of cyclo-[GGG]kB1[T] indicate that this region is disordered and this was confirmed in the 3D structure of cyclo-[GGG]kB1[T] (Fig. 4A). The solution structure was calculated using CYANA (60) followed by refinement in a water shell using CNS (63) based on 388 NOE distance restraints, 53 dihedral angle restraints, including 26 ϕ , 20 ψ

and 6 χ_1 dihedral angle restraints and 5 hydrogen bonds derived from temperature coefficient data (Table 1). The 20 conformers with the lowest energy superimposed with a backbone root mean square deviation (RMSD) of 0.53 ± 0.14 Å across residues 1-24 (Fig. 4A). Comparison of the cyclo-[GGG]kB1[T] structure with that of native kB1 (PDB ID: 1NB1) shows them to be very similar except for the more flexible loop 6 of cyclo-[GGG]kB1[T] is (Fig. 4B).

Hemolytic activity and serum stability assay of cyclo-[GGG]kB1[T]- Native kB1 possesses mild hemolytic activity (15,51), which is undesired in a pharmaceutical context. Thus, to assess the effects of SrtA cyclization on the novel kB1 analogue, the hemolytic activity of cyclo-[GGG]kB1[T] and linear oxidized [GGG]kB1[TGG] was determined and compared with the native peptide. Compared to native kB1 both peptides exhibited significantly less hemolytic activity (Fig. 5A). After 24 h incubation, 50 μ M of native kB1 lysed 64% of human erythrocytes whereas in the same time period only 6% or 2% of erythrocytes were lysed by the same concentration of cyclo-[GGG]kB1[T] or linear oxidized [GGG]kB1[TGG], respectively. The reduced hemolytic activity is consistent with previous mutagenesis studies on kB1, which showed that linearization or strategic replacement of certain residues can abrogate hemolytic activity (72,73).

To determine the effects of SrtA-mediated cyclization on the stability of the peptide, cyclo-[GGG]kB1[T] was incubated in human serum. Encouragingly, its stability was comparable to that of native kB1, with only a slight reduction in peptide survival observed. After a 24 h incubation, 77.4% and 95.9% of the starting concentration of cyclo-[GGG]kB1[T] and kB1 respectively was still present (Fig. 5B). Interestingly, 71% of linear oxidized [GGG]kB1[TGG] also remained in human serum after 24 h. In contrast, a linear 12-mer control peptide, without any disulfide bond, was completely degraded within the first hour.

Oxidation and cyclization of [G]Vc1.1[GLPETGGS]- α -conotoxin Vc1.1 was

successfully synthesized with a SrtA sorting motif at the C-terminus and an additional Gly residue at the N-terminus. AcM protecting groups on Cys4 and Cys17 were used for selective disulfide bond formation of Cys^{II}-Cys^{IV} (Fig. 6A). As for cyclo-[GGG]kB1[T], two approaches, namely oxidation prior to cyclization or cyclization prior to oxidation, were attempted to obtain the cyclo-[G]Vc1.1[GLPET]. The former approach gave rise to only a low yield (~1%) of oxidized product following AcM removal. In contrast, isomerization during oxidative folding was averted by cyclizing the linear precursor [G]Vc1.1[GLPETGGS] prior to oxidation. The cyclization performed in the presence of 10 mM TCEP resulted in one major product with ~50% yield. The two disulfide bonds in the cyclic reduced [G]Vc1.1[GLPET] were then successfully formed via a two-step oxidation process with ~15% yield. The linear precursor [G]Vc1.1[GLPETGGS], cyclic reduced [G]Vc1.1[GLPET] and cyclic oxidized [G]Vc1.1[GLPET] (hereafter named cyclo-[G]Vc1.1[GLPET]) showed a change in retention time after each reaction (Fig. 6B). The molecular mass and purity of the desired products for each step were confirmed by MALDI-TOF and RP-HPLC (Fig. 6B).

NMR analysis of cyclo-[G]Vc1.1[GLPET]- The structure of cyclo-[G]Vc1.1[GLPET] was deduced using secondary H α chemical shifts determined from TOCSY and NOESY spectra. A comparison of the secondary shifts of cyclo-[G]Vc1.1[GLPET] with both native and chemically cyclized Vc1.1 (3) suggested no significant difference in the overall structure. Cyclization of cyclo-[G]Vc1.1[GLPET] was confirmed by observation of a sequential H α -NH_{i+1} NOE between the C- and N-termini.

SrtA reaction for SFTI-1- For this single disulfide-bonded peptide the SrtA reaction was performed at pH 8.5 to achieve cyclization and oxidation in a one-pot reaction. After 9 h, ~70% of the linear precursor had been converted to the cyclic oxidized form based on the RP-HPLC profile (peak at 20 min, Fig. 6C). The mass of cyclic oxidized [GG]SFTI-1[LPET] was

This is a post-print version of the following article: Jia, Xinying, Kwon, Soohyun, Wang, Ching-I Anderson, Huang, Yen-Hua, Chan, Lai Y., Tan, Chia Chia, Rosengren, K. Johan, Mulvenna, Jason P., Schroeder, Christina I. and Craik, David J. (2014) Semiozymatic cyclization of disulfide-rich peptides using sortase A. *Journal of Biological Chemistry, Papers in Press* : 1-25.

confirmed by MALDI-TOF (Fig. 6C). After 24 h incubation the peak at 20 min decreased and a peak at 22.8 min increased in height and was found to contain both cyclic oxidized and hydrolysed linear [GG]SFTI-1[LPET].

NMR analysis of cyclo-[GG]SFTI-1[LPET]-Purified cyclized and oxidized cyclo-[GG]SFTI-1[LPET] and wild type SFTI-1 (both peptides >95% pure) were analysed using TOCSY and NOESY experiments. Two distinct conformations, in an approximate 9:1 ratio, were observed for cyclo-[GG]SFTI-1[LPET]. The secondary shifts of the major conformation were almost identical with those of wild type SFTI-1 (Fig. 6D). The minor conformation appears to be due to *cis-trans* isomerisation of a proline residue. Pro8 in wild type SFTI-1 is in the *cis*-conformation, with a strong NOEs observed between Ile7 H α to Pro8 H α_{i+1} . By contrast, in cyclo-[GG]SFTI-1[LPET] two sets of NOEs interacting with either δ -proton or α -proton of Pro8 were observed, suggesting that Pro8 exists in both *cis* and *trans* conformations (49).

DISCUSSION

Disulfide-rich cyclic peptides offer an attractive framework for the development of stable bioactive peptides with pharmaceutical potential. They display a remarkable degree of functional plasticity and high stability. Accordingly, interest has been shown both in the cyclization of linear disulfide-rich peptides (especially those isolated from venoms), as well as the development of native cyclotides as therapeutics and in their use as scaffolds for the grafting of pharmaceutically relevant epitopes onto the native cyclotide framework (74,75). A bottleneck in the development of these peptides as potential therapeutics, though, is the production of linear precursors and their subsequent cyclization and folding. NCL (using Boc-chemistry) has been the preferred strategy for the production of disulfide-rich cyclic peptides, but this approach requires reaction conditions that cannot always be achieved using Fmoc chemistry or recombinantly expressed

proteins. We therefore investigated SrtA-mediated cyclization as a mechanism for the increased efficiency of one of the steps in cyclic peptide production, namely head-to-tail cyclization of synthetically produced peptides. Specifically, we explored the possibility of using SrtA to enzymatically cyclize SFTI-1, Vc1.1 (with a linker) and kB1, and showed that SrtA offers an efficient, safe and cost-effective method for the cyclization of disulfide-rich peptides ranging in size from 14 to 29 amino acids with 1-3 disulfide bonds.

The presence of a native Leu-Pro-Val in loop 6 of kB1 made this peptide an ideal model for cyclization using SrtA. These three residues fortuitously form a part of the penta-amino acid sorting motif, LPXTG, and cyclization was achieved with minimal disruption to the native sequence of kB1. In NCL-based synthesis of kB1, the cyclization and oxidation is carried out in a one-pot fashion. However, the reaction requires a two-step procedure when using SrtA for cyclization, with oxidation occurring either after or before SrtA mediated cyclization. In our hands, the order of the reaction, i.e. oxidation/cyclization vs cyclization/oxidation, had a significant effect on the yield of correctly folded peptide. Despite the minimal changes introduced in kB1 by SrtA cyclization no correctly folded peptide was produced when oxidation occurred after cyclization. Small changes in the amino acid composition of cyclotides can have profound effects on the refolding of synthetic forms (6,20) and it is possible that the introduction of the TGGG amino acid sequence in loop 6 of kB1 had a negative effect on the oxidative refolding of the cyclic form. The proximity of the cyclization point to Cys¹ (Fig. 1) might also have adversely affected oxidative folding. The only region of significant structural perturbation in cyclo-[GGG]kB1[T] was for the Leu-Pro-Val residues immediately preceding Cys¹ and, when combined with restraints imposed by cyclization, conformational variations in this region of the reduced, cyclized peptide might have prevented correct disulfide formation.

Production of correctly folded cyclo-

This is a post-print version of the following article: Jia, Xinying, Kwon, Soohyun, Wang, Ching-I Anderson, Huang, Yen-Hua, Chan, Lai Y., Tan, Chia Chia, Rosengren, K. Johan, Mulvenna, Jason P., Schroeder, Christina I. and Craik, David J. (2014) Semiozymatic cyclization of disulfide-rich peptides using sortase A. *Journal of Biological Chemistry, Papers in Press* : 1-25.

[GGG]kB1[T] was achieved by oxidative refolding prior to cyclization with SrtA. Monitoring of the cyclization reaction showed what appeared to be intermediates at various stages of the reaction, (Fig. 2B) but by 24 h the reaction had efficiently converted the linear peptides to the cyclic form in ~49% yield.

Several pieces of NMR evidence support that cyclo-[GGG]kB1[T] adopts the fold of native kB1: (i) Pro20 adopts a *cis*-conformation as in native kB1; (ii) The HN of Trp19 is not observed in TOCSY spectra but is observed in NOESY spectra, as characteristically applies to kB1; (iii) The HB of Pro20 is shifted upfield to -0.26 ppm; (iv) The protonation/deprotonation of Glu3 significantly affects the chemical shifts of HN of Asn11 and Thr12; (v) The χ_1 dihedral angles of all six cysteines residues agree with those for kB1, providing strong evidence for an identical disulfide connectivity. Consistent with this connectivity, NOEs between Cys1 H β 2/H β 3 to Cys15 H β 3 and Cys10 H β 2/H β 3 to Cys22 H β 2 were observed (NOEs between Cys5 H β and Cys17 H β could not be unambiguously identified due to extensive spectral overlap). Interestingly, NOEs between H β protons of non-connected cysteine residues, including Cys10-Cys15, Cys1-Cys22 and Cys15-Cys22 were also observed, but this is in complete accordance with a study on native kB1 by Rosengren *et al* (54) where it was suggested that for cyclic cystine knot peptides, H β cross-peaks are not the preferred diagnostic tool for determining disulfide connectivity due to the close proximity of all disulfide bonds. From the extensive evidence noted above, especially the fact that the two peptides share identical χ_1 dihedral angles for all the Cys residues, we were confident that we produced cyclo-[GGG]kB1[T] with the native disulfide connectivity. Thus, we calculated the structure of cyclo-GGGkB1T using the cysteine connectivities as native kB1 (PDB ID: 1NB1).

The hemolytic activity of cyclo-[GGG]kB1[T] was significantly reduced compared to native kB1. As structural perturbation of cyclo-[GGG]kB1[T]

was minimal (Fig. 5) the loss of hemolytic activity is presumably due to the effects of the residues introduced into loop 6 upon cyclization. Previous grafting experiments utilising kB1 have also shown the abrogation of hemolytic activity after relatively minor changes to the primary sequence; for example the grafting of the vascular endothelial growth factor sequence (RRKRRR) into loops 2, 3, 5, or 6 significantly reduced the hemolytic activity of kB1 (20). The effects of single point mutations on the hemolytic activity of kB1 have also been extensively studied (73). The hemolytic activity of kB1 was dramatically reduced by Ala substitution on a specific set of residues, including the last three residues of loop 6 (Leu27, Pro28 and Val29). Similar results were observed during Lys substitution at the same positions (69). Barry *et al* (72) also noted complete loss of hemolytic activity of linearized kB1 with RNGLP sequence deletion. All the studies suggest that the hemolytic activity of kB1 can be diminished when a less hydrophobic residue is introduced into the last three positions of loop 6. In kalata B2, a close homolog of kB1, loop 6 forms part of a hydrophobic interface that mediates interactions between the cyclotide and the plasma membrane (76). In this context, the loss of hemolytic activity after the introduction of additional residues to loop 6 suggests the interruption of critical membrane/peptide interactions in this region of the peptide.

The residues introduced into loop 6 might have also contributed to the slight reduction in stability of cyclo-[GGG]kB1[T] relative to the native peptide. Chemical shifts for these residues differed little from random coil values, suggesting that structural disorder at the cyclization point made the peptide slightly more susceptible to plasma proteases than native kB1. This disorder was also confirmed in the NMR solution structure of [GGG]kB1[T], with loop 6 displaying markedly increased disorder compared to native kB1. The serum stability results show that the cystine knot formation is crucial for stability as linear oxidized [GGG]kB1[TGG] was largely (~71%) intact after

This is a post-print version of the following article: Jia, Xinying, Kwon, Soohyun, Wang, Ching-I Anderson, Huang, Yen-Hua, Chan, Lai Y., Tan, Chia Chia, Rosengren, K. Johan, Mulvenna, Jason P., Schroeder, Christina I. and Craik, David J. (2014) Semienzymatic cyclization of disulfide-rich peptides using sortase A. *Journal of Biological Chemistry, Papers in Press* : 1-25.

24 h.

The sortase-catalyzed process requires modest modifications in order to render peptides amenable to cyclization. In this work the cyclization point was chosen on the basis of a pre-existing Leu-Pro-Val motif in loop 6 which overlapped with the SrtA recognition motif. This fortuitous coincidence resulted in the introduction of three fewer non-native amino acids than would be required using a different cyclization point. Analysis of chemical shifts showed that apart from differences of ~0.5 ppm in the Leu-Pro-Val residues of the cyclization point, the remainder of the SrtA cyclized peptide exhibited very little structural perturbation. Loop 6 of cyclotides exhibits the greatest diversity in structure, sequence and length (77) and the lack of structural perturbation in this case reflects the ability of this loop to accommodate a range of structural motifs without affecting the overall fold of the peptide. Accordingly, the use of this loop for cyclization should provide a convenient and simple mechanism for production of synthetic cyclotides for a variety of applications.

To test the generality of SrtA-mediated cyclization we investigated if it could be applied to other small disulfide-rich peptides such as α -conotoxin Vc1.1 and SFTI-1. MALDI-TOF and NMR analysis confirmed that their cyclized and oxidized structures were similar to the native structures. In contrast to kB1, 9 h of SrtA reaction appeared to be sufficient to obtain the maximum yield for cyclo-[GG]SFTI-1[LPET], presumably due to its smaller size. Beyond this incubation time, some hydrolysis of the peptide was found to occur, resulting in linearization since the final product still contains a LPETG motif. Interestingly, introduction of the sortase-motif in SFTI-1 (cyclo-[GG]SFTI-1[LPET]), gave rise to *cis-trans* isomerization of Pro8, as highlighted by the observation of strong NOEs between both Ile7H α_i – Pro8H α_{i+1} (*cis*) and Ile7H α_i – Pro8H δ_{i+1} (*trans*). Although the LPXTG motif was introduced to the cyclic loop of SFTI-1, presumably placing the motif next to the Asp14 made structure of the

peptide less constrained than the wild type. This is consistent with a previous study showing that Ile7, Pro8, Pro9 and Asp14 are important for structural integrity (49). In that study, when Asp14 was replaced with Ala the turn region was destabilized, resulting in *cis-trans* isomerization of Pro13 (49). Even though the isomerization site is different, introduction of the SrtA sorting motif appears to have destabilized the turn region, giving rise to the minor conformation observed by NMR.

The work described here demonstrates the applicability of the SrtA method for the cyclization of different classes of disulfide-rich peptides without significant structural perturbation to the overall peptide fold. We have shown that this method is applicable whether the peptides are cyclic in their native form such as SFTI-1 containing one disulfide-bond, or kB1 with a three disulfide-bond cyclic cystine knot motif or whether the peptide is linear in its native form and the cyclization site is introduced by the addition of a linker, such as for cVc1.1. SrtA-mediated head-to-tail cyclization, works optimally with peptides larger than 12-mers, excluding the SrtA sorting signal (40). Cyclotides are typically 28-37 amino acids in size, making all characterized cyclotides suitable for SrtA cyclization. In addition, other disulfide-rich peptides, for example conotoxins (78) or defensins (79,80), are also within this size range, making SrtA mediated cyclization a possibility for a wide range of peptides of therapeutic interest. Importantly, the ability to place the SrtA tags at any position within a peptide sequence makes it possible to introduce cyclization points anywhere in the peptide of interest and thus minimise disruption of biologically or structurally important motifs. Thus peptide bond closure of linear precursors through sortase-catalysed circularization represents a simple, safe and effective method, not only for the production of synthetic cyclotides, but also for the introduction of increased stability and bioavailability to other disulfide-rich peptides with therapeutic value.

This is a post-print version of the following article: Jia, Xinying, Kwon, Soohyun, Wang, Ching-I Anderson, Huang, Yen-Hua, Chan, Lai Y., Tan, Chia Chia, Rosengren, K. Johan, Mulvenna, Jason P., Schroeder, Christina I. and Craik, David J. (2014) Semiozymatic cyclization of disulfide-rich peptides using sortase A. *Journal of Biological Chemistry, Papers in Press* : 1-25.

REFERENCES

1. Colgrave, M. L., and Craik, D. J. (2004) Thermal, chemical, and enzymatic stability of the cyclotide kalata B1: The importance of the cyclic cystine knot. *Biochemistry* **43**, 5965-5975
2. Gran, L. (1970) An oxytocic principle found in *Oldenlandia affinis* DC. An indigenous, Congolese drug "Kalata-Kalata" used to accelerate delivery. *Medd. Nor. Farm. Selsk.* **32**, 173-180
3. Clark, R. J., Jensen, J., Nevin, S. T., Callaghan, B. P., Adams, D. J., and Craik, D. J. (2010) The engineering of an orally active conotoxin for the treatment of neuropathic pain. *Angew. Chem. Int. Ed. Engl.* **49**, 6545-6548
4. Wong, C. T., Rowlands, D. K., Wong, C. H., Lo, T. W., Nguyen, G. K., Li, H. Y., and Tam, J. P. (2012) Orally active peptidic bradykinin B1 receptor antagonists engineered from a cyclotide scaffold for inflammatory pain treatment. *Angew. Chem. Int. Ed. Engl.* **51**, 5620-5624
5. Cemazar, M., Kwon, S., Mahatmanto, T., Ravipati, A. S., and Craik, D. J. (2012) Discovery and applications of disulfide-rich cyclic peptides. *Curr. Top. Med. Chem.* **12**, 1534-1545
6. Clark, R. J., Fischer, H., Dempster, L., Daly, N. L., Rosengren, K. J., Nevin, S. T., Meunier, F. A., Adams, D. J., and Craik, D. J. (2005) Engineering stable peptide toxins by means of backbone cyclization: stabilization of the alpha-conotoxin MII. *Proc. Natl. Acad. Sci. U. S. A.* **102**, 13767-13772
7. Luckett, S., Garcia, R. S., Barker, J. J., Konarev, A. V., Shewry, P. R., Clarke, A. R., and Brady, R. L. (1999) High-resolution structure of a potent, cyclic proteinase inhibitor from sunflower seeds. *J. Mol. Biol.* **290**, 525-533
8. Long, Y. Q., Lee, S. L., Lin, C. Y., Enyedy, I. J., Wang, S., Li, P., Dickson, R. B., and Roller, P. P. (2001) Synthesis and evaluation of the sunflower derived trypsin inhibitor as a potent inhibitor of the type II transmembrane serine protease, matriptase. *Bioorg. Med. Chem. Lett.* **11**, 2515-2519
9. Craik, D. J., Daly, N. L., Bond, T., and Waive, C. (1999) Plant cyclotides: A unique family of cyclic and knotted proteins that defines the cyclic cystine knot structural motif. *J. Mol. Biol.* **294**, 1327-1336
10. Trabi, M., and Craik, D. J. (2002) Circular proteins - no end in sight. *Trends Biochem. Sci.* **27**, 132-138
11. Jennings, C., West, J., Waive, C., Craik, D., and Anderson, M. (2001) Biosynthesis and insecticidal properties of plant cyclotides: The cyclic knotted proteins from *Oldenlandia affinis*. *Proc. Natl. Acad. Sci. U. S. A.* **98**, 10614-10619
12. Jennings, C. V., Rosengren, K. J., Daly, N. L., Plan, M., Stevens, J., Scanlon, M. J., Waive, C., Norman, D. G., Anderson, M. A., and Craik, D. J. (2005) Isolation, solution structure, and insecticidal activity of kalata B2, a circular protein with a twist: Do Mobius

This is a post-print version of the following article: Jia, Xinying, Kwon, Soohyun, Wang, Ching-I Anderson, Huang, Yen-Hua, Chan, Lai Y., Tan, Chia Chia, Rosengren, K. Johan, Mulvenna, Jason P., Schroeder, Christina I. and Craik, David J. (2014) Semienzymatic cyclization of disulfide-rich peptides using sortase A. *Journal of Biological Chemistry, Papers in Press* : 1-25.

- strips exist in nature? *Biochemistry* **44**, 851-860
13. Plan, M. R. R., Saska, I., Cagauan, A. G., and Craik, D. J. (2008) Backbone cyclised peptides from plants show molluscicidal activity against the rice pest *Pomacea canaliculata* (golden apple snail). *J. Agric. Food Chem.* **56**, 5237-5241
 14. Gustafson, K. R., Sowder, R. C., Henderson, L. E., Parsons, I. C., Kashman, Y., Cardellina, J. H., McMahon, J. B., Buckheit Jr, R. W., Pannell, L. K., and Boyd, M. R. (1994) Circulins A and B. Novel human immunodeficiency virus (HIV)-inhibitory macrocyclic peptides from the tropical tree *Chassalia parvifolia*. *J. Am. Chem. Soc.* **116**, 9337-9338
 15. Tam, J. P., Lu, Y. A., Yang, J. L., and Chiu, K. W. (1999) An unusual structural motif of antimicrobial peptides containing end-to-end macrocycle and cystine-knot disulfides. *Proc. Natl. Acad. Sci. U. S. A.* **96**, 8913-8918
 16. Gruber, C. W., Cemazar, M., Anderson, M. A., and Craik, D. J. (2007) Insecticidal plant cyclotides and related cystine knot toxins. *Toxicon* **49**, 561-575
 17. Lindholm, P., Goransson, U., Johansson, S., Claeson, P., Gullbo, J., Larsson, R., Bohlin, L., and Backlund, A. (2002) Cyclotides: A novel type of cytotoxic agents. *Mol. Cancer Ther.* **1**, 365-369
 18. Svargard, E., Goransson, U., Hocaoglu, Z., Gullbo, J., Larsson, R., Claeson, P., and Bohlin, L. (2004) Cytotoxic cyclotides from *Viola tricolor*. *J. Nat. Prod.* **67**, 144-147
 19. Kaas, Q., and Craik, D. J. (2010) Analysis and classification of circular proteins in CyBase. *Biopolymers* **94**, 584-591
 20. Gunasekera, S., Foley, F. M., Clark, R. J., Sando, L., Fabri, L. J., Craik, D. J., and Daly, N. L. (2008) Engineering stabilized vascular endothelial growth factor-A antagonists: Synthesis, structural characterization, and bioactivity of grafted analogues of cyclotides. *J. Med. Chem.* **51**, 7697-7704
 21. Thongyoo, P., Roque-Rosell, N., Leatherbarrow, R. J., and Tate, E. W. (2008) Chemical and biomimetic total syntheses of natural and engineered MCoTI cyclotides. *Org. Biomol. Chem.* **6**, 1462-1470
 22. Thongyoo, P., Bonomelli, C., Leatherbarrow, R. J., and Tate, E. W. (2009) Potent inhibitors of β -tryptase and human leukocyte elastase based on the MCoTI-II scaffold. *J. Med. Chem.* **52**, 6197-6200
 23. Chan, L. Y., Gunasekera, S., Henriques, S. T., Worth, N. F., Le, S. J., Clark, R. J., Campbell, J. H., Craik, D. J., and Daly, N. L. (2011) Engineering pro-angiogenic peptides using stable, disulfide-rich cyclic scaffolds. *Blood* **118**, 6709-6717
 24. Ji, Y., Majumder, S., Millard, M., Borra, R., Bi, T., Elnagar, A. Y., Neamati, N., Shekhtman, A., and Camarero, J. A. (2013) In vivo activation of the p53 tumor suppressor pathway by an engineered cyclotide. *J. Am. Chem. Soc.* **135**, 11623-11633
 25. Contreras, J., Elnagar, A. Y., Hamm-Alvarez, S. F., and Camarero, J. A. (2011) Cellular uptake of cyclotide MCoTI-I follows multiple endocytic pathways. *J. Control. Release* **155**, 134-143
 26. Greenwood, K. P., Daly, N. L., Brown, D. L., Stow, J. L., and Craik, D. J. (2007) The

This is a post-print version of the following article: Jia, Xinying, Kwon, Soohyun, Wang, Ching-I Anderson, Huang, Yen-Hua, Chan, Lai Y., Tan, Chia Chia, Rosengren, K. Johan, Mulvenna, Jason P., Schroeder, Christina I. and Craik, David J. (2014) Semienzymatic cyclization of disulfide-rich peptides using sortase A. *Journal of Biological Chemistry, Papers in Press* : 1-25.

- cyclic cystine knot miniprotein MCoTI-II is internalized into cells by macropinocytosis. *Int. J. Biochem. Cell Biol.* **39**, 2252-2264
27. Cascales, L., Henriques, S. T., Kerr, M. C., Huang, Y. H., Sweet, M. J., Daly, N. L., and Craik, D. J. (2011) Identification and characterization of a new family of cell-penetrating peptides. *J. Biol. Chem.* **286**, 36932-36943
 28. Henriques, S. T., Huang, Y. H., Rosengren, K. J., Franquelim, H. G., Carvalho, F. A., Johnson, A., Sonza, S., Tachedjian, G., Castanho, M. A., Daly, N. L., and Craik, D. J. (2011) Decoding the membrane activity of the cyclotide kalata B1: the importance of phosphatidylethanolamine phospholipids and lipid organization on hemolytic and anti-HIV activities. *J. Biol. Chem.* **286**, 24231-24241
 29. Aboye, T. L., and Camarero, J. A. (2012) Biological synthesis of circular polypeptides. *J. Biol. Chem.* **287**, 27026-27032
 30. Pattabiraman, V. R., and Bode, J. W. (2011) Rethinking amide bond synthesis. *Nature* **480**, 471-479
 31. Clark, R. J., and Craik, D. J. (2010) Native chemical ligation applied to the synthesis and bioengineering of circular peptides and proteins. *Biopolymers* **94**, 414-422
 32. Dawson, P. E., Muir, T. W., Clark-Lewis, I., and Kent, S. B. (1994) Synthesis of proteins by native chemical ligation. *Science* **266**, 776-779
 33. Kimura, R., and Camarero, J. A. (2005) Expressed protein ligation: a new tool for the biosynthesis of cyclic polypeptides. *Protein Pept. Lett.* **12**, 789-794
 34. Muir, T. W. (2003) Semisynthesis of proteins by expressed protein ligation. *Annu. Rev. Biochem.* **72**, 249-289
 35. Tavassoli, A., and Benkovic, S. J. (2007) Split-intein mediated circular ligation used in the synthesis of cyclic peptide libraries in *E. coli*. *Nat. Protoc.* **2**, 1126-1133
 36. Kawakami, T., Ohta, A., Ohuchi, M., Ashigai, H., Murakami, H., and Suga, H. (2009) Diverse backbone-cyclized peptides via codon reprogramming. *Nat. Chem. Biol.* **5**, 888-890
 37. Parthasarathy, R., Subramanian, S., and Boder, E. T. (2007) Sortase A as a novel molecular "stapler" for sequence-specific protein conjugation. *Bioconjug. Chem.* **18**, 469-476
 38. Antos, J. M., Popp, M. W., Ernst, R., Chew, G. L., Spooner, E., and Ploegh, H. L. (2009) A straight path to circular proteins. *J. Biol. Chem.* **284**, 16028-16036
 39. Bolscher, J. G., Oudhoff, M. J., Nazmi, K., Antos, J. M., Guimaraes, C. P., Spooner, E., Haney, E. F., Garcia Vallejo, J. J., Vogel, H. J., van't Hof, W., Ploegh, H. L., and Veerman, E. C. (2011) Sortase A as a tool for high-yield histatin cyclization. *FASEB J.* **25**, 2650-2658
 40. Wu, Z., Guo, X., and Guo, Z. (2011) Sortase A-catalyzed peptide cyclization for the synthesis of macrocyclic peptides and glycopeptides. *Chem. Commun.* **47**, 9218-9220
 41. Mazmanian, S. K., Liu, G., Ton-That, H., and Schneewind, O. (1999) *Staphylococcus aureus* sortase, an enzyme that anchors surface proteins to the cell wall. *Science* **285**, 760-763

This is a post-print version of the following article: Jia, Xinying, Kwon, Soohyun, Wang, Ching-I Anderson, Huang, Yen-Hua, Chan, Lai Y., Tan, Chia Chia, Rosengren, K. Johan, Mulvenna, Jason P., Schroeder, Christina I. and Craik, David J. (2014) Semienzymatic cyclization of disulfide-rich peptides using sortase A. *Journal of Biological Chemistry, Papers in Press* : 1-25.

42. Popp, M. W., and Ploegh, H. L. (2011) Making and breaking peptide bonds: protein engineering using sortase. *Angew. Chem. Int. Ed. Engl.* **50**, 5024-5032
43. Marraffini, L. A., DeDent, A. C., and Schneewind, O. (2006) Sortases and the art of anchoring proteins to the envelopes of gram-positive bacteria. *Microbiol. Mol. Biol. Rev.* **70**, 192-221
44. Ton-That, H., Liu, G., Mazmanian, S. K., Faull, K. F., and Schneewind, O. (1999) Purification and characterization of sortase, the transpeptidase that cleaves surface proteins of *Staphylococcus aureus* at the LPXTG motif. *Proc. Natl. Acad. Sci. U. S. A.* **96**, 12424-12429
45. Antos, J. M., Chew, G. L., Guimaraes, C. P., Yoder, N. C., Grotenbreg, G. M., Popp, M. W., and Ploegh, H. L. (2009) Site-specific N- and C-terminal labeling of a single polypeptide using sortases of different specificity. *J. Am. Chem. Soc.* **131**, 10800-10801
46. Popp, M. W., Dougan, S. K., Chuang, T. Y., Spooner, E., and Ploegh, H. L. (2011) Sortase-catalyzed transformations that improve the properties of cytokines. *Proc. Natl. Acad. Sci. U. S. A.* **108**, 3169-3174
47. Ling, J. J., Policarpo, R. L., Rabideau, A. E., Liao, X., and Pentelute, B. L. (2012) Protein thioester synthesis enabled by sortase. *J. Am. Chem. Soc.* **134**, 10749-10752
48. Witte, M. D., Cragolini, J. J., Dougan, S. K., Yoder, N. C., Popp, M. W., and Ploegh, H. L. (2012) Preparation of unnatural N-to-N and C-to-C protein fusions. *Proc. Natl. Acad. Sci. U. S. A.* **109**, 11993-11998
49. Daly, N. L., Chen, Y. K., Foley, F. M., Bansal, P. S., Bharathi, R., Clark, R. J., Sommerhoff, C. P., and Craik, D. J. (2006) The absolute structural requirement for a proline in the P3'-position of Bowman-Birk protease inhibitors is surmounted in the minimized SFTI-1 scaffold. *J. Biol. Chem.* **281**, 23668-23675
50. Popp, M. W., Antos, J. M., and Ploegh, H. L. (2009) Site-specific protein labeling via sortase-mediated transpeptidation. *Curr. Protoc. Protein. Sci*, **Chapter 15**, Unit 15 13
51. Daly, N. L., Love, S., Alewood, P. F., and Craik, D. J. (1999) Chemical synthesis and folding pathways of large cyclic polypeptide: Studies of the cystine knot polypeptide kalata B1. *Biochemistry* **38**, 10606-10614
52. Huang, Y. H., Colgrave, M. L., Daly, N. L., Keleshian, A., Martinac, B., and Craik, D. J. (2009) The biological activity of the prototypic cyclotide kalata B1 is modulated by the formation of multimeric pores. *J. Biol. Chem.* **284**, 20699-20707
53. Moffatt, F., Senkans, P., and Ricketts, D. (2000) Approaches towards the quantitative analysis of peptides and proteins by reversed-phase high-performance liquid chromatography in the absence of a pure reference sample. *J. Chromatogr. A* **891**, 235-242
54. Rosengren, K. J., Daly, N. L., Plan, M. R., Waine, C., and Craik, D. J. (2003) Twists, knots, and rings in proteins - Structural definition of the cyclotide framework. *J. Biol. Chem.* **278**, 8606-8616
55. Hwang, T. L., and Shaka, A. J. (1995) Water suppression that works. Excitation sculpting using arbitrary wave-forms and pulsed-field gradients. *J. Magn. Reson.* **112**, 275-279

This is a post-print version of the following article: Jia, Xinying, Kwon, Soohyun, Wang, Ching-I Anderson, Huang, Yen-Hua, Chan, Lai Y., Tan, Chia Chia, Rosengren, K. Johan, Mulvenna, Jason P., Schroeder, Christina I. and Craik, David J. (2014) Semienzymatic cyclization of disulfide-rich peptides using sortase A. *Journal of Biological Chemistry, Papers in Press* : 1-25.

56. Griesinger, C., Sørensen, O. W., and Ernst, R. R. (1987) Practical aspects of the E.COSY technique. Measurement of scalar spin-spin coupling constants in peptides. *J. Magn. Reson.* **75**, 474-492
57. Vranken, W. F., Boucher, W., Stevens, T. J., Fogh, R. H., Pajon, A., Llinas, M., Ulrich, E. L., Markley, J. L., Ionides, J., and Laue, E. D. (2005) The CCPN data model for NMR spectroscopy: development of a software pipeline. *Proteins* **59**, 687-696
58. Bartels, C., Xia, T. H., Billeter, M., Guntert, P., and Wuthrich, K. (1995) The program XEASY for computer-supported NMR spectral analysis of biological macromolecules. *J. Biomol. NMR* **6**, 1-10
59. Wishart, D. S., Bigam, C. G., Yao, J., Abildgaard, F., Dyson, H. J., Oldfield, E., Markley, J. L., and Sykes, B. D. (1995) ¹H, ¹³C and ¹⁵N chemical shift referencing in biomolecular NMR. *J. Biomol. NMR* **6**, 135-140
60. Guntert, P. (2004) Automated NMR structure calculation with CYANA. *Methods Mol. Biol.* **278**, 353-378
61. Shen, Y., Delaglio, F., Cornilescu, G., and Bax, A. (2009) TALOS+: a hybrid method for predicting protein backbone torsion angles from NMR chemical shifts. *J. Biomol. NMR* **44**, 213-223
62. Nederveen, A. J., Doreleijers, J. F., Vranken, W., Miller, Z., Spronk, C. A., Nabuurs, S. B., Guntert, P., Livny, M., Markley, J. L., Nilges, M., Ulrich, E. L., Kaptein, R., and Bonvin, A. M. (2005) RECOORD: a recalculated coordinate database of 500+ proteins from the PDB using restraints from the BioMagResBank. *Proteins* **59**, 662-672
63. Brunger, A. T., Adams, P. D., Clore, G. M., DeLano, W. L., Gros, P., Grosse-Kunstleve, R. W., Jiang, J. S., Kuszewski, J., Nilges, M., Pannu, N. S., Read, R. J., Rice, L. M., Simonson, T., and Warren, G. L. (1998) Crystallography & NMR system: A new software suite for macromolecular structure determination. *Acta Crystallogr. D Biol. Crystallogr.* **54**, 905-921
64. Dominguez, C., Boelens, R., and Bonvin, A. M. (2003) HADDOCK: a protein-protein docking approach based on biochemical or biophysical information. *J. Am. Chem. Soc.* **125**, 1731-1737
65. Linge, J. P., and Nilges, M. (1999) Influence of non-bonded parameters on the quality of NMR structures: a new force field for NMR structure calculation. *J. Biomol. NMR* **13**, 51-59
66. Conibear, A. C., Rosengren, K. J., Harvey, P. J., and Craik, D. J. (2012) Structural characterization of the cyclic cystine ladder motif of theta-defensins. *Biochemistry* **51**, 9718-9726
67. Chen, V. B., Arendall, W. B., Headd, J. J., Keedy, D. a., Immormino, R. M., Kapral, G. J., Murray, L. W., Richardson, J. S., and Richardson, D. C. (2010) MolProbity: all-atom structure validation for macromolecular crystallography. *Acta Crystallogr. D Biol. Crystallogr.* **66**, 12-21
68. Koradi, R., Billeter, M., and Wuthrich, K. (1996) MOLMOL: a program for display and analysis of macromolecular structures. *J. Mol. Graph.* **14**, 51-55, 29-32

This is a post-print version of the following article: Jia, Xinying, Kwon, Soohyun, Wang, Ching-I Anderson, Huang, Yen-Hua, Chan, Lai Y., Tan, Chia Chia, Rosengren, K. Johan, Mulvenna, Jason P., Schroeder, Christina I. and Craik, David J. (2014) Semienzymatic cyclization of disulfide-rich peptides using sortase A. *Journal of Biological Chemistry, Papers in Press* : 1-25.

69. Huang, Y. H., Colgrave, M. L., Clark, R. J., Kotze, A. C., and Craik, D. J. (2010) Lysine-scanning mutagenesis reveals an amendable face of the cyclotide kalata B1 for the optimization of nematocidal activity. *J. Biol. Chem.* **285**, 10797-10805
70. Levary, D. A., Parthasarathy, R., Boder, E. T., and Ackerman, M. E. (2011) Protein-protein fusion catalyzed by sortase A. *PLoS ONE* **6**, e18342
71. Wüthrich, K. (1986) NMR of proteins and nucleic acids, Wiley-Interscience, New York.
72. Barry, D. G., Daly, N. L., Clark, R. J., Sando, L., and Craik, D. J. (2003) Linearization of a naturally occurring circular protein maintains structure but eliminates hemolytic activity. *Biochemistry* **42**, 6688-6695
73. Simonsen, S. M., Sando, L., Rosengren, K. J., Wang, C. K., Colgrave, M. L., Daly, N. L., and Craik, D. J. (2008) Alanine scanning mutagenesis of the prototypic cyclotide reveals a cluster of residues essential for bioactivity. *J. Biol. Chem.* **283**, 9805-9813
74. Craik, D. J., Swedberg, J. E., Mylne, J. S., and Cemazar, M. (2012) Cyclotides as a basis for drug design. *Expert Opin. Drug Deliv.* **7**, 179-194
75. Gould, A., Ji, Y., Aboye, T. L., and Camarero, J. A. (2011) Cyclotides, a novel ultrastable polypeptide scaffold for drug discovery. *Curr. Pharm. Des.* **17**, 4294-4307
76. Wang, C. K., Colgrave, M. L., Ireland, D. C., Kaas, Q., and Craik, D. J. (2009) Despite a conserved cystine knot motif, different cyclotides have different membrane binding modes. *Biophys. J.* **97**, 1471-1481
77. Mulvenna, J. P. R., Sando, L., and Craik, D. J. (2005) Processing of a 22 kDa precursor protein to produce the circular protein tricyclon A. *Structure* **13**, 691-701
78. Terlau, H., and Olivera, B. M. (2004) Conus venoms: a rich source of novel ion channel-targeted peptides. *Physiol. Rev.* **84**, 41-68
79. Ganz, T. (2003) Defensins: antimicrobial peptides of innate immunity. *Nat. Rev. Immunol.* **3**, 710-720
80. Wong, J. H., Xia, L., and Ng, T. B. (2007) A review of defensins of diverse origins. *Curr. Protein Pept. Sci.* **8**, 446-459
81. Wishart, D. S., Bigam, C. G., Holm, a., Hodges, R. S., and Sykes, B. D. (1995) ¹H, ¹³C and ¹⁵N random coil NMR chemical shifts of the common amino acids. I. Investigations of nearest-neighbor effects. *J. Biomol. NMR* **5**, 67-81
82. Davis, I. W., Leaver-Fay, A., Chen, V. B., Block, J. N., Kapral, G. J., Wang, X., Murray, L. W., Arendall, W. B., 3rd, Snoeyink, J., Richardson, J. S., and Richardson, D. C. (2007) MolProbity: all-atom contacts and structure validation for proteins and nucleic acids. *Nucleic Acids Res.* **35**, W375-383

This is a post-print version of the following article: Jia, Xinying, Kwon, Soohyun, Wang, Ching-I Anderson, Huang, Yen-Hua, Chan, Lai Y., Tan, Chia Chia, Rosengren, K. Johan, Mulvenna, Jason P., Schroeder, Christina I. and Craik, David J. (2014) Semienzymatic cyclization of disulfide-rich peptides using sortase A. *Journal of Biological Chemistry, Papers in Press* : 1-25.

Acknowledgements - We thank Dr. Maximilian Wei-Lin Popp and Prof. Hidde L. Ploegh from the Whitehead Institute for Biomedical Research for providing the SrtA expression plasmids.

FOOTNOTES

*This work was supported by Australian National Health and Medical Research Council (NHMRC) Project grant APP1047857. The authors acknowledge financial support provided by the Queensland State Government to the Queensland NMR Network facilities at The University of Queensland.

¹ These two authors contributed equally to this work.

² JPM and KJR are supported by Career Development Awards (CDA) from the Australian NHMRC.

³ To whom correspondence should be addressed. David J. Craik or Christina I. Schroeder, The University of Queensland, Institute for Molecular Bioscience, Brisbane 4072, Qld, Australia. Tel.: 61-7-33462019; Fax: 61-7-33462101; E-mail: d.craik@imb.uq.edu.au or c.schroeder@imb.uq.edu.au.

⁴ DJC is an Australian NHMRC Professorial Fellow (APP1026501).

⁵ The structure of [GGG]kB1[T] has been submitted to the Protein Data Bank (PDB ID: 2MH1) and the Biological Magnetic Resonance Data Bank (BMRB ID: 19611).

⁶ The abbreviations used are: SrtA, sortaseA; SFTI-1, sunflower trypsin inhibitor 1; CCK, cyclic cystine knot; NCL, native chemical ligation; SPPS, solid phase peptide synthesis; BOC, *t*-butoxycarbonyl; Fmoc, fluorenylmethyloxycarbonyl; AcM, acetamidomethyl; TIPS, triisopropylsilane; ACN, acetonitrile; DSS, 2,2-dimethyl-2-silapentane-5-sulfonate; RT, room temperature; IPTG, β -D-thiogalactopyranoside; RP-HPLC, reversed-phase high performance liquid chromatography; MALDI-TOF, matrix absorbance laser direct inject – time of flight; NMR, nuclear magnetic resonance; TOCSY, total correlation spectroscopy; NOESY, nuclear Overhauser enhancement spectroscopy; DQF-COSY, double-quantum filtered-correlated spectroscopy; HSQC, heteronuclear single quantum coherence spectroscopy; E.COSY, exclusive correlation spectroscopy; NOE, nuclear Overhauser effect; PBS phosphate-buffered saline; kB1, kalata B1; TCEP, tris(2-carboxyethyl)phosphine; RMSD, root mean square deviation.

This is a post-print version of the following article: Jia, Xinying, Kwon, Soohyun, Wang, Ching-I Anderson, Huang, Yen-Hua, Chan, Lai Y., Tan, Chia Chia, Rosengren, K. Johan, Mulvenna, Jason P., Schroeder, Christina I. and Craik, David J. (2014) Semienzymatic cyclization of disulfide-rich peptides using sortase A. *Journal of Biological Chemistry, Papers in Press* : 1-25.

FIGURE LEGENDS

FIGURE 1. (A) Representation of the sequence and structure (PDB ID: 1JBL) of native SFTI-1, (B) native kalata B1 (PDB ID: 1NB1) (kB1) which is the prototypic cyclotide, (C) native linear Vc1.1 (PDB ID: 2H8S) which has been cyclized by a 6-amino acid linker using native chemical ligation (3,32). The disulfide bonding network is shown as sticks, with the cysteine residues numbered. Amino acids are represented by their one-letter code. (D) The linear oxidized [GGG]kB1[TGG] contains a SrtA recognition sequence (LPVTG) and undergoes an intramolecular transpeptidation reaction catalyzed by SrtA to form cyclic oxidized [GGG]kB1[T] (cyclo-[GGG]kB1[T]).

FIGURE 2. (A) RP-HPLC profile of [GGG]kB1[TGG] oxidation at 0 and 20 h. A major peak of linear precursor peptide and linear oxidized product is marked with schematic representation of the peptide. (B) Time course analysis of the SrtA reaction progress monitored by RP-HPLC. Aliquots were taken from the reaction mixture at 0, 4, 8, 12 and 24 h, and loaded onto an analytical RP-HPLC. (C) MALDI-TOF analysis of linear precursor, linear oxidized [GGG]kB1[TGG], native kB1 peptide and cyclic oxidized [GGG]kB1[T] (clockwise). Cyclo-[GGG]kB1[T] revealed a mass corresponding to the linear oxidized [GGG]kB1[TGG] minus two glycines and a water molecule, indicative of the formation of an amide bond between the N- and the C-terminal. (D) Analytical RP-HPLC profile of purified cyclo-[GGG]kB1[T] (above) and co-injection of cyclo-[GGG]kB1[T] and native kB1 (below) to demonstrate their only slightly different retention times.

FIGURE 3. H_{α} secondary shift comparison of native kB1 (empty squares with dashed line) and cyclo-[GGG]kB1[T] (filled squares with solid line). The H_{α} secondary shifts were calculated by subtracting random coil shifts (81) from the experimental H_{α} shifts. The box highlights loop 6, where the extra residues TGGG were introduced by the SrtA-mediated cyclization.

FIGURE 4. (A) Superimposition of the 20 lowest energy structures of cyclo-[GGG]kB1[T] shown in blue with disulfide bonds shown in orange. (B) Comparison of cyclo-[GGG]kB1[T] in blue with native kB1 in red (PDB ID: 1NB1) by superimposition of residues 1-24 of cyclo-[GGG]kB1[T] against residues 1-24 of the native kB1 structure. Disulfide bonds shown in orange highlighting the similarities between the two structures across loop 1-5 and the increased flexibility of loop 6 by insertion of the SrtA sorting-motif. RMSD across heavy backbone atoms for residues 1-24 cyclo-[GGG]kB1[T] / 1-24 kB1 is 0.461.

FIGURE 5. Hemolytic and serum-stability assay on cyclo-[GGG]kB1[T]. (A) Percentage of hemolysis by cyclo-[GGG]kB1[T] compared to native kB1 included as a positive control. (B) Percentage of peptide remaining after 0, 1, 2, 3, 5, 8, 11 and 24 h incubation in human serum. The data are presented as means \pm standard deviation (SD).

Figure 6. (A) Cyclization strategy for [G]Vc1.1[GLPETGGS] and [GG]SFTI-1[LPETGG] by SrtA. (B) Retention time and MALDI-TOF analysis of linear precursor [G]Vc1.1[GLPETGGS], cyclic reduced and cyclic oxidized [G]Vc1.1[LPET]. The peptide status is shown with schematic representations. (C) One-pot reaction of oxidation and cyclization of [GG]SFTI-1[LPETGG]. Time course analysis of SrtA reaction by RP-HPLC (left), MALDI-TOF data (right) of linear precursor [GG]SFTI-1[LPETGG] and cyclic oxidized(cyclo)-[GG]SFTI-1[LPET]. (D) H_{α} secondary shift comparison of cyclo-[GG]SFTI-1[LPET] and wild type SFTI-1. (E) H_{α} secondary shift comparison of cyclo-[G]Vc1.1[GLPET], wild

This is a post-print version of the following article: Jia, Xinying, Kwon, Soohyun, Wang, Ching-I Anderson, Huang, Yen-Hua, Chan, Lai Y., Tan, Chia Chia, Rosengren, K. Johan, Mulvenna, Jason P., Schroeder, Christina I. and Craik, David J. (2014) Semienzymatic cyclization of disulfide-rich peptides using sortase A. *Journal of Biological Chemistry, Papers in Press* : 1-25.

type Vc1.1, and the orally active analgesic peptide cVc1.1 (3). The sorting motif is shown in a dashed box.

Table 1: Energies and structural statistics for the family of 20 lowest energy cyclo-[GGG]kB1[T] structures^a.

Energies (kcal/mol)	
Overall	-975.7 ± 38.5
Bonds	20.5 ± 1.4
Angles	52.5 ± 4.3
Improper	17.4 ± 2.3
Van der Waals	-96.1 ± 4.7
NOE	0.3 ± 0.03
cDih	0.3 ± 0.2
Dihedral	129.7 ± 1.6
Electrostatic	-1100.3 ± 36.4
MolProbity Statistics	
Clashes (>0.4 Å / 1000 atoms)	12.8 ± 4.1
Poor rotamers	0.3 ± 0.4
Ramachandran Outliers (%)	0.0 ± 0.0
Ramachandran Favoured (%) ^b	87.6 ± 2.7
MolProbity score	2.3 ± 0.2
MolProbity score percentile	56.2 ± 13.4 ^c
Atomic RMSD^d (Å)	
Mean global backbone (1-24)	0.53 ± 0.14
Mean global heavy (1-24)	1.11 ± 0.25
Mean global backbone (1-33)	1.53 ± 0.58
Mean global heavy (1-33)	1.90 ± 0.53
Distance Restraints	
Intraresidue (i-j = 0)	59
Sequential (/i-j/ = 1)	169
Medium range (/i-j/ < 5)	53
Long range (/i-j/ > 5)	107
Hydrogen bonds	10
Total	398
Dihedral angle restraints	
φ	26

This is a post-print version of the following article: Jia, Xinying, Kwon, Soohyun, Wang, Ching-I Anderson, Huang, Yen-Hua, Chan, Lai Y., Tan, Chia Chia, Rosengren, K. Johan, Mulvenna, Jason P., Schroeder, Christina I. and Craik, David J. (2014) Semienzymatic cyclization of disulfide-rich peptides using sortase A. *Journal of Biological Chemistry, Papers in Press* : 1-25.

Ψ	20
χ^1	6
Total	53

Violations from experimental restraints

Total NOE violations exceeding 0.3 Å	0
Total Dihedral violations exceeding 3.0°	0

^a Based on structures with highest overall MolProbity score (82).

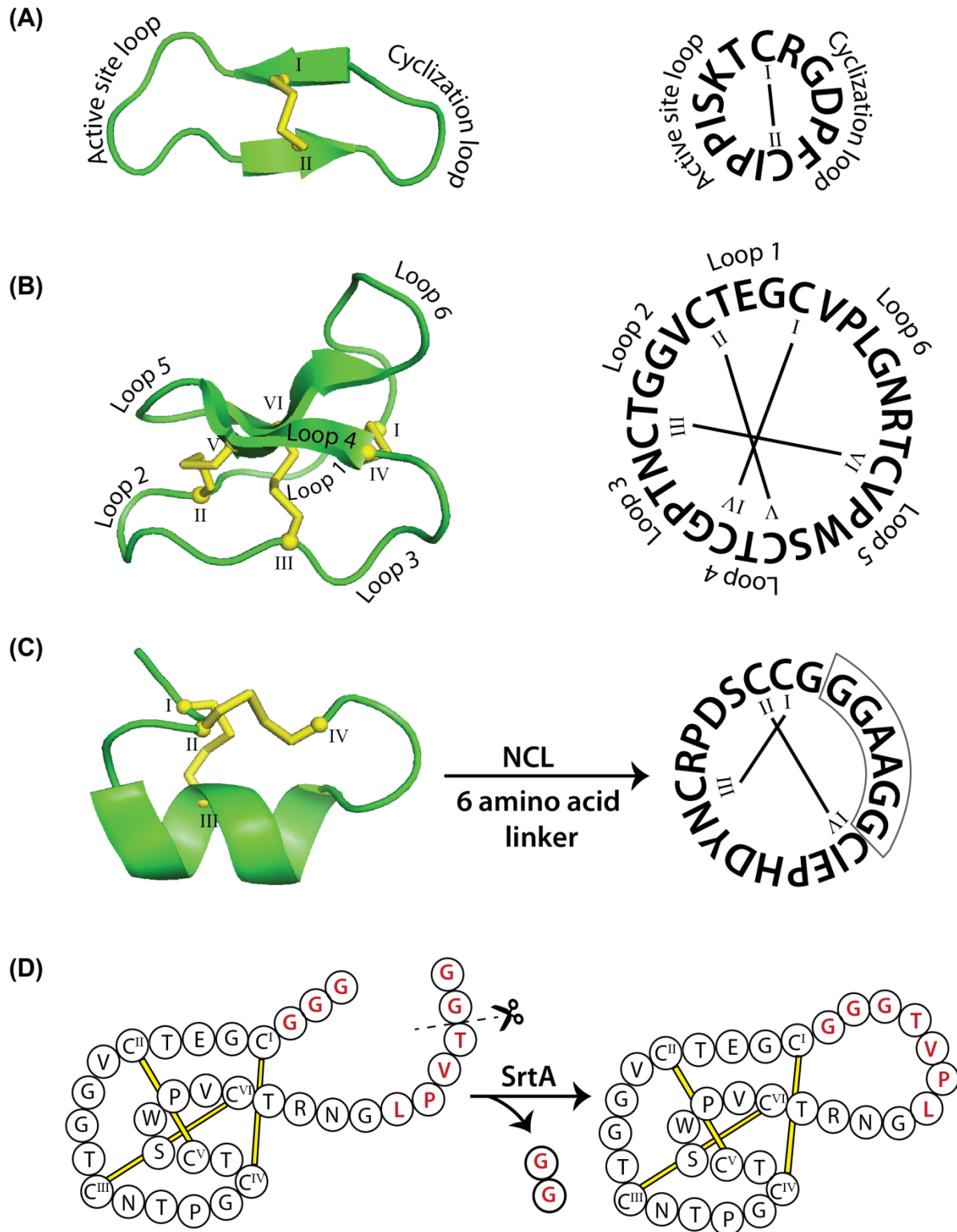
^b The remaining 12.4% are found in the allowed regions of the Ramachandran plot.

^c 100th percentile is the best among structures of comparable resolution; 0th percentile is the worst.

^d RMSD calculated using MOLMOL (68).

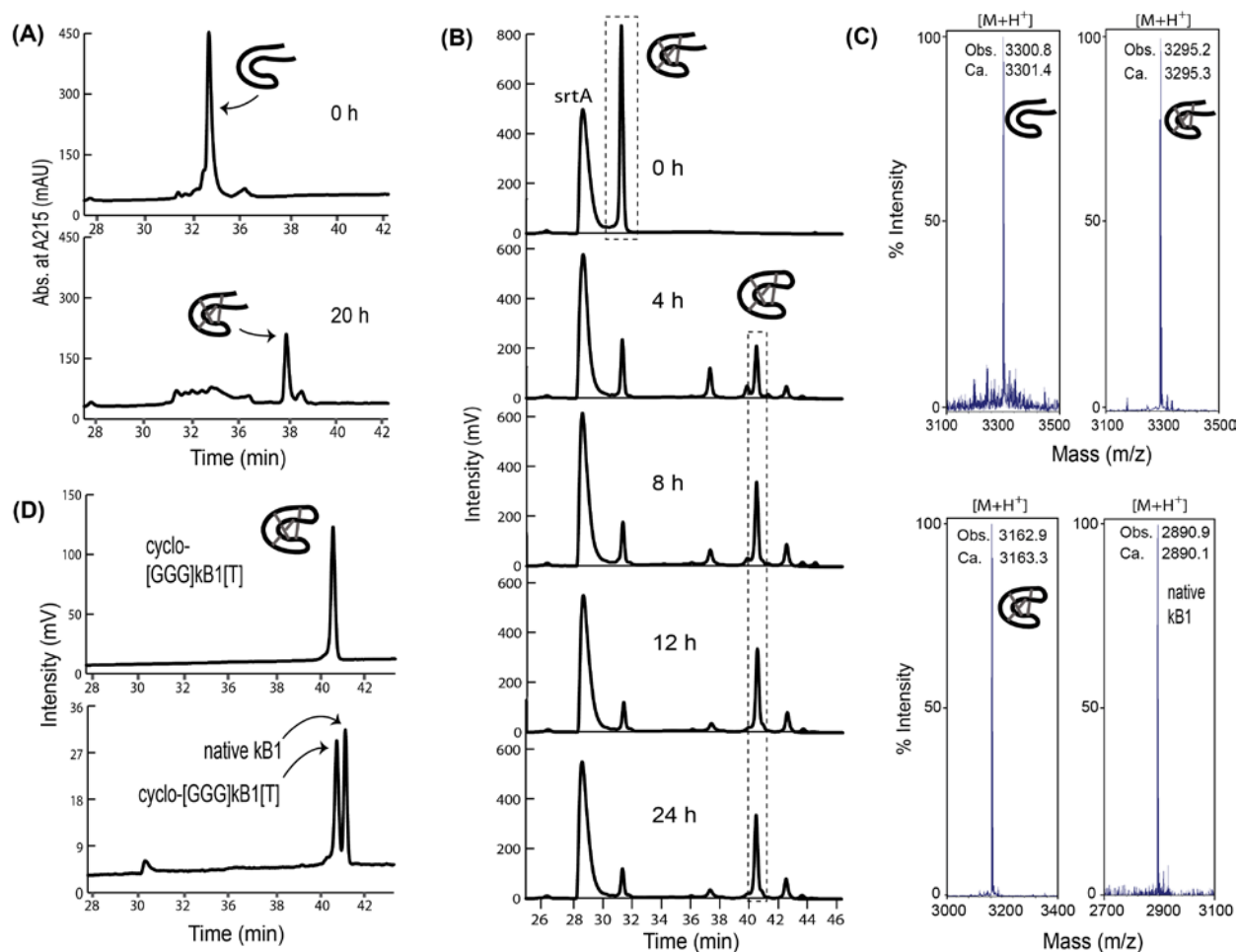
Figure 1.

This is a post-print version of the following article: Jia, Xinying, Kwon, Soohyun, Wang, Ching-I Anderson, Huang, Yen-Hua, Chan, Lai Y., Tan, Chia Chia, Rosengren, K. Johan, Mulvenna, Jason P., Schroeder, Christina I. and Craik, David J. (2014) Semienzymatic cyclization of disulfide-rich peptides using sortase A. *Journal of Biological Chemistry, Papers in Press* : 1-25.



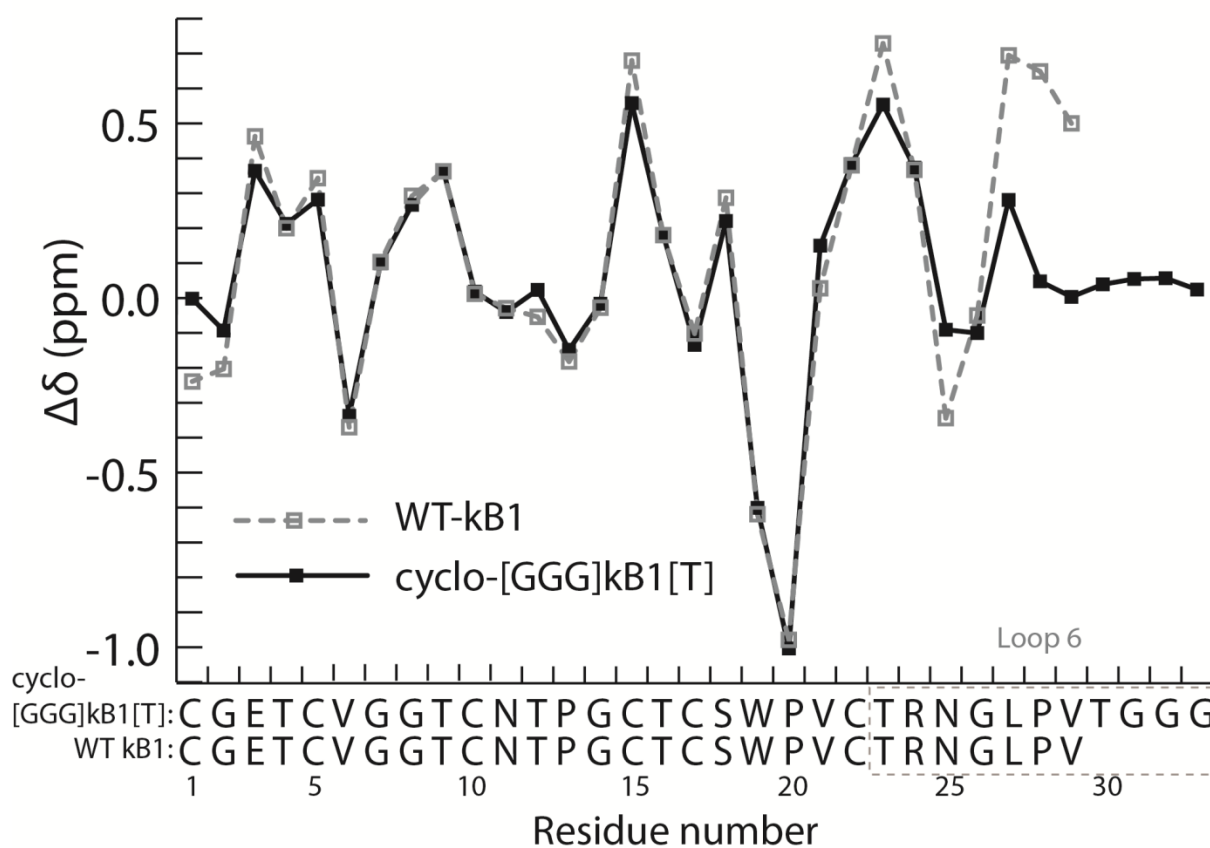
Yen-Hua, Chan, Lai Y., Tan, Chia Chia, Rosengren, K. Johan, Mulvenna, Jason P., Schroeder, Christina I. and Craik, David J. (2014) Semienzymatic cyclization of disulfide-rich peptides using sortase A. *Journal of Biological Chemistry, Papers in Press* : 1-25.

Figure 2.



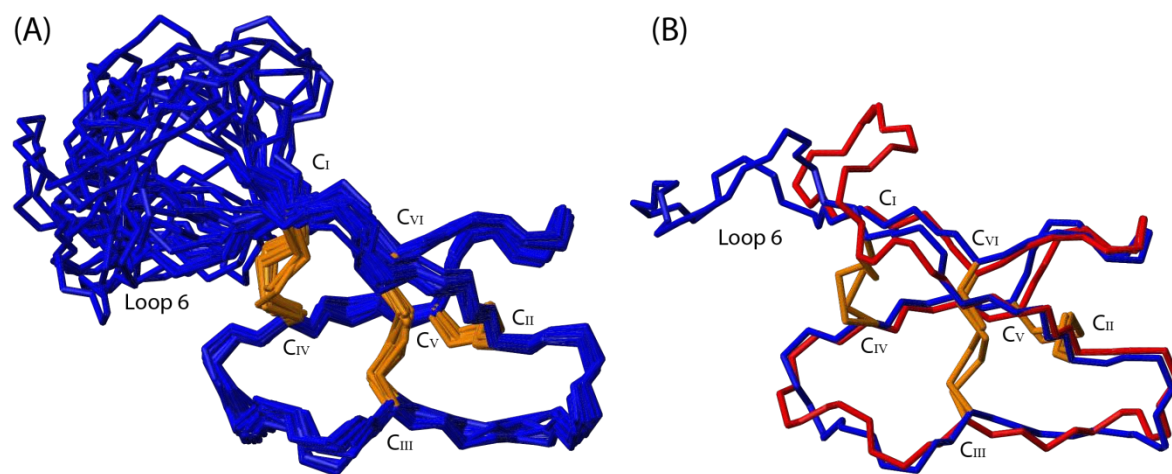
This is a post-print version of the following article: Jia, Xinying, Kwon, Soohyun, Wang, Ching-I Anderson, Huang, Yen-Hua, Chan, Lai Y., Tan, Chia Chia, Rosengren, K. Johan, Mulvenna, Jason P., Schroeder, Christina I. and Craik, David J. (2014) Semienzymatic cyclization of disulfide-rich peptides using sortase A. *Journal of Biological Chemistry, Papers in Press* : 1-25.

Figure 3.



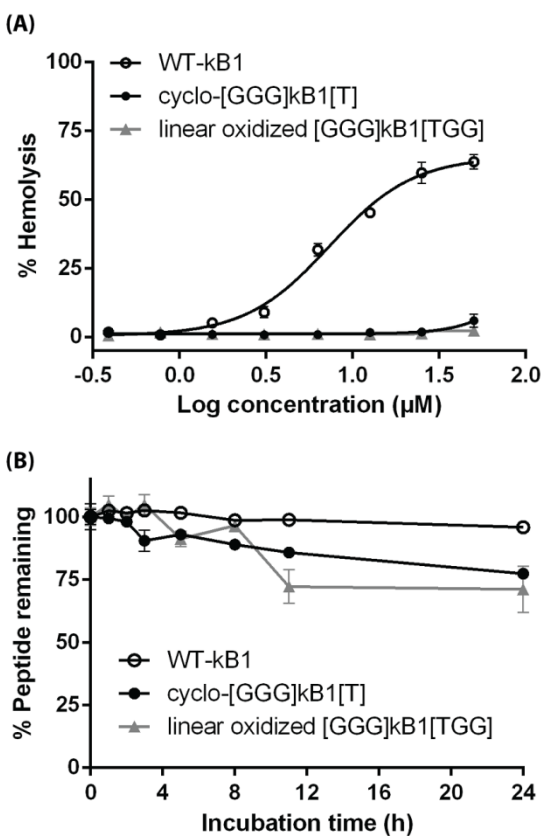
This is a post-print version of the following article: Jia, Xinying, Kwon, Soohyun, Wang, Ching-I Anderson, Huang, Yen-Hua, Chan, Lai Y., Tan, Chia Chia, Rosengren, K. Johan, Mulvenna, Jason P., Schroeder, Christina I. and Craik, David J. (2014) Semienzymatic cyclization of disulfide-rich peptides using sortase A. *Journal of Biological Chemistry, Papers in Press* : 1-25.

Figure 4.



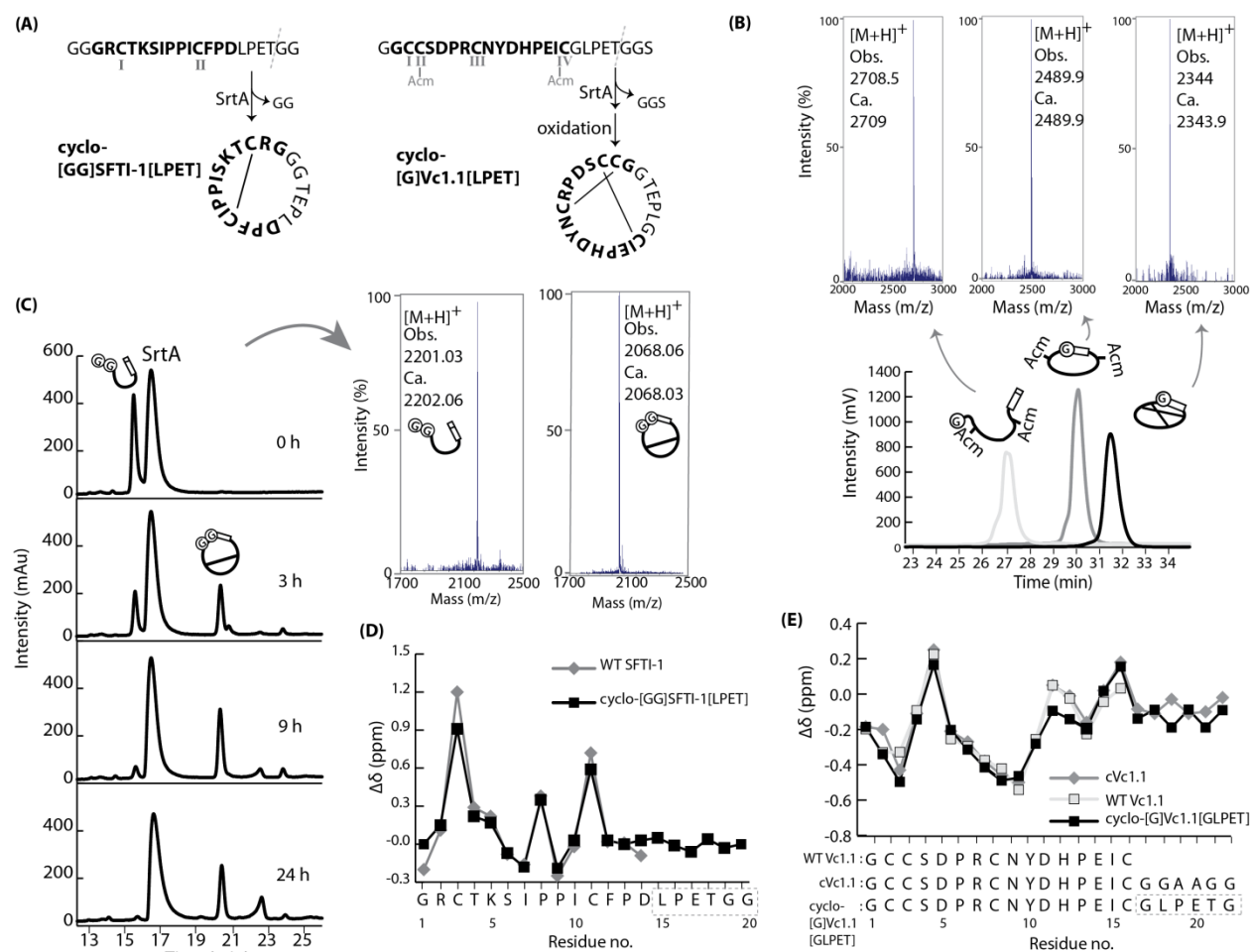
This is a post-print version of the following article: Jia, Xinying, Kwon, Soohyun, Wang, Ching-I Anderson, Huang, Yen-Hua, Chan, Lai Y., Tan, Chia Chia, Rosengren, K. Johan, Mulvenna, Jason P., Schroeder, Christina I. and Craik, David J. (2014) Semienzymatic cyclization of disulfide-rich peptides using sortase A. *Journal of Biological Chemistry, Papers in Press* : 1-25.

Figure 5.



This is a post-print version of the following article: Jia, Xinying, Kwon, Soohyun, Wang, Ching-I Anderson, Huang, Yen-Hua, Chan, Lai Y., Tan, Chia Chia, Rosengren, K. Johan, Mulvenna, Jason P., Schroeder, Christina I. and Craik, David J. (2014) Semienzymatic cyclization of disulfide-rich peptides using sortase A. *Journal of Biological Chemistry, Papers in Press* : 1-25.

Figure 6.



This is a post-print version of the following article: Jia, Xinying, Kwon, Soohyun, Wang, Ching-I Anderson, Huang, Yen-Hua, Chan, Lai Y., Tan, Chia Chia, Rosengren, K. Johan, Mulvenna, Jason P., Schroeder, Christina I. and Craik, David J. (2014) Semienzymatic cyclization of disulfide-rich peptides using sortase A. *Journal of Biological Chemistry, Papers in Press* : 1-25.

Supplemental data

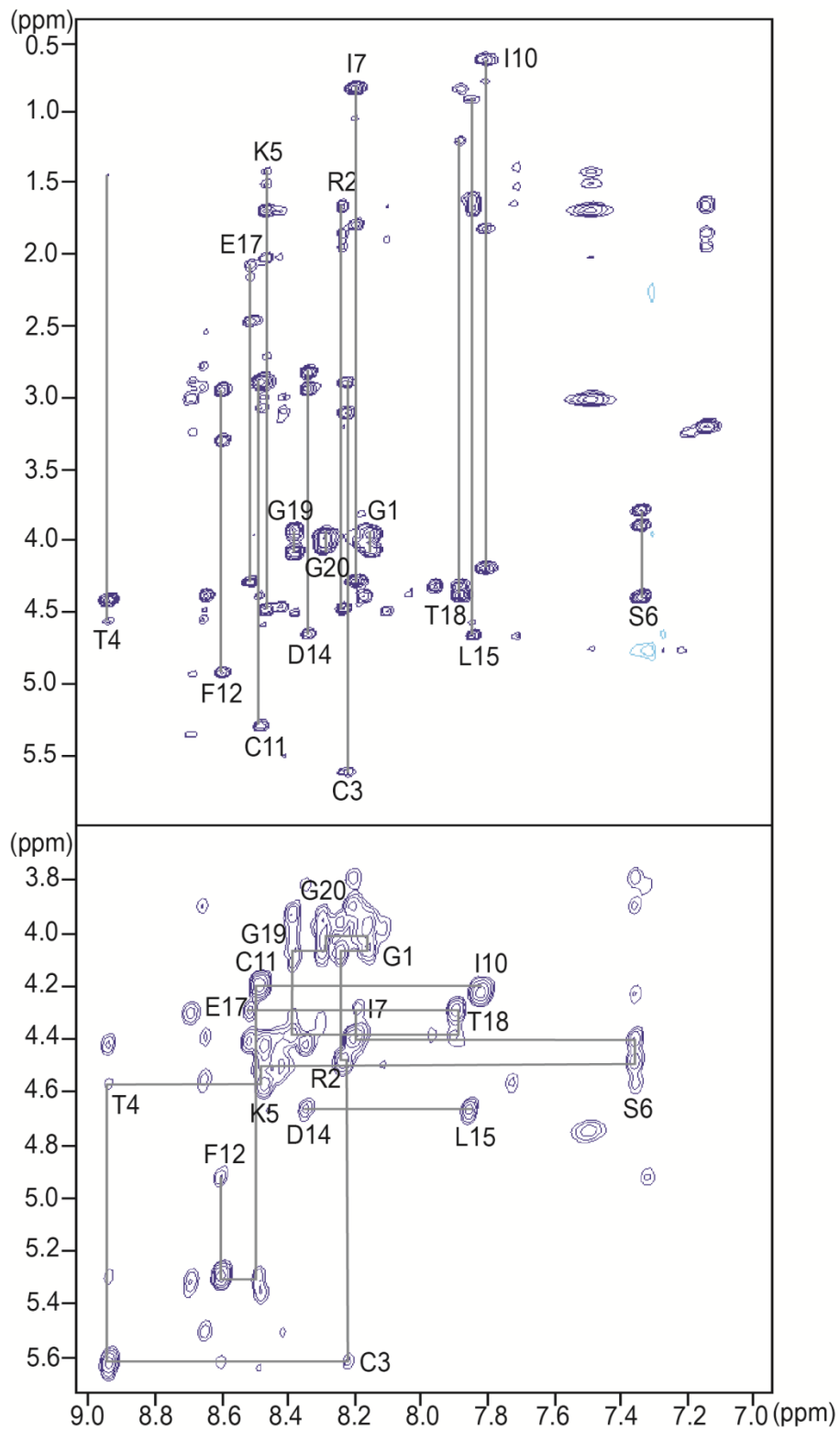
Title: Semienzymatic cyclization of disulfide-rich peptides using sortase A.

Xinying Jia^{†‡1}, Soohyun Kwon^{‡1}, Ching-I Anderson Wang[‡], Yen-Hua Huang[‡], Lai Y. Chan[‡], Chia Chia Tan[‡], K. Johan Rosengren^{§2}, Jason P. Mulvenna^{†2}, Christina I. Schroeder^{‡3}, David J. Craik^{‡3,4}

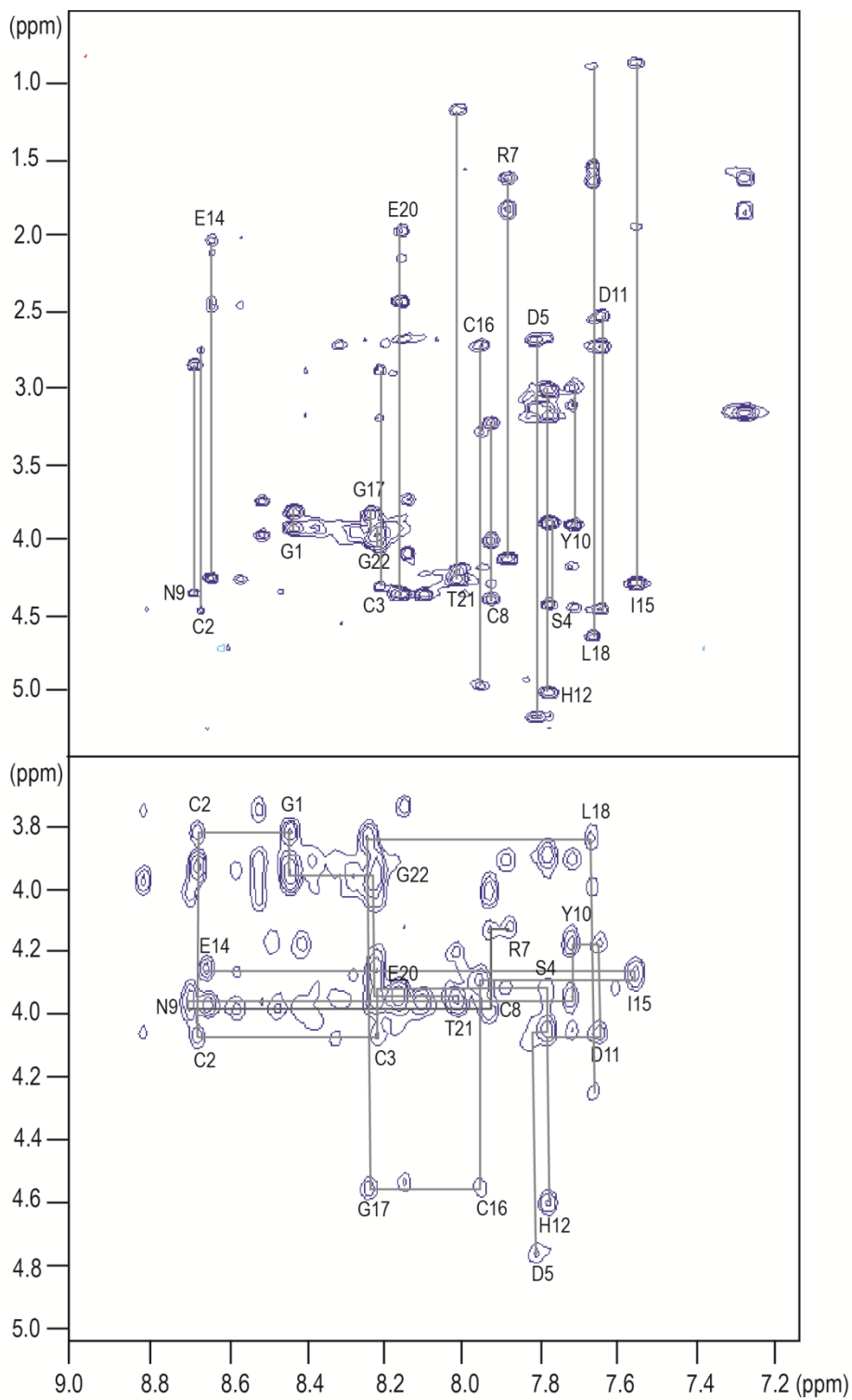
[†]QIMR Berghofer Medical Research, Brisbane 4000, Qld, Australia.

[‡]The University of Queensland, Institute for Molecular Bioscience, Brisbane 4072, Qld, Australia

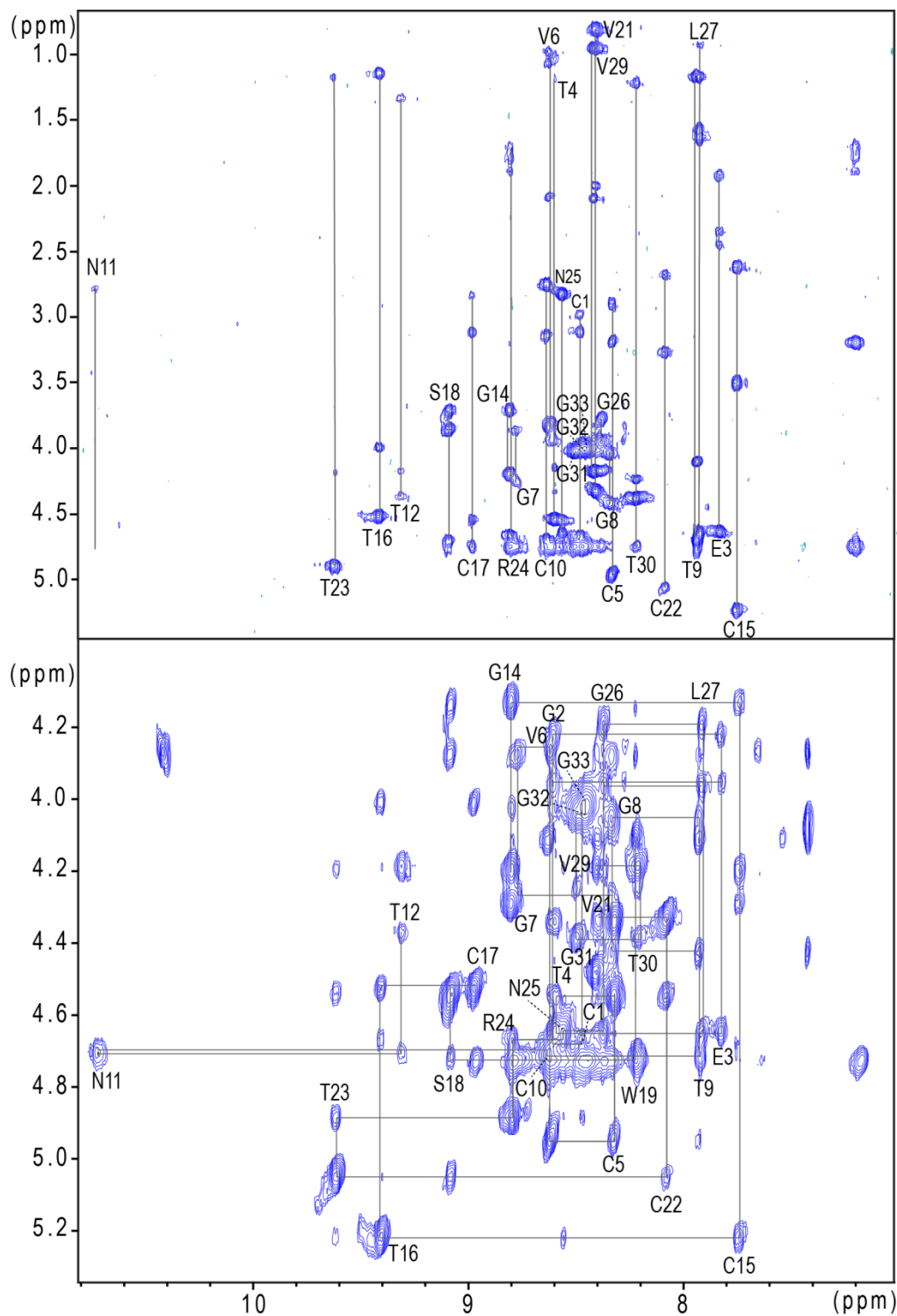
[§]The University of Queensland, School of Biomedical Sciences, Brisbane 4072, Qld, Australia



NMR spectra of cyclo-[GG]SFTI-1[LPET]. TOCSY spectrum (upper panel) and NOESY spectrum (lower panel) recorded at 298K, 90% H₂O/10% D₂O.



NMR spectra of cyclo-[G]Vc1.1[GLPET]. TOCSY spectrum (upper panel) and NOESY spectrum (lower panel) recorded at 298K, 90% H₂O/10% D₂O. There was a subset of extra residues found to be from Gly1 to Ser4 and Glu14 to Gly22 with overlapping or similar chemical shifts to the major conformer. This is caused by *cis-trans* isomerization of Pro19 in the linker (GLPETG), but it did not affect the overall structure of cyclo-[G]Vc1.1[GLPET].



TOCSY (the upper panel) and NOESY (the lower panel, the enlarged HA region) spectrum of cyclo-[GGG]kB1[T] recorded at 298 K, 90% H₂O/10% D₂O. The upper panel shows the spin systems by vertical lines, except Trp19 which was not observable in the TOCSY, while the lower panel highlights the sequential walk, except for Pro13, Pro20 and Pro28.